

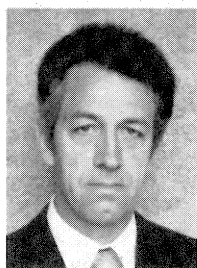
STEAM TURBINE BLADE DESIGN OPTIONS: HOW TO SPECIFY OR UPGRADE

by

Helmut G. Naumann

Turbomachinery Consultant

Skillman, New Jersey



Helmut G. Naumann holds a degree of Diplom Ingenieur in Turbomachinery Design from the Technical University, Braunschweig, Germany, and a M.S. and Ph.D. in Mechanical Engineering from the University of Pennsylvania in Philadelphia, Pennsylvania.

His experience encompasses steel manufacturing with Krupp, Germany, for one year and gas turbine design with Westinghouse Electric Corporation for two years. He has taught Mechanical Engineering subjects full time for eight years at Widener University and part time at University of Pennsylvania, Rutgers University, and Widener University for five years. In specification, installation, maintenance and troubleshooting of turbomachinery he has had experience as a Supervisor with Atlantic Richfield Company for six years and as a Manager with Brown Boveri Company for two years. He is a member of ASME.

Since July 1981 he has conducted an independent turbomachinery consulting practice.

ABSTRACT

This paper is intended to familiarize people, who are responsible for rotating equipment, with options in blade designs. The information is meant to be helpful in conjunction with blade specifications, design reviews, inspection and troubleshooting.

Mechanisms of causes of blade fatigue and strength deterioration are reviewed. With emphasis on these factors, geometrical and manufacturing differences of blade fastenings, lashings and shrouds are discussed and a qualitative method of identifying stress distributions and stress concentrations in root cross sections is presented.

Graphs in tabular form coordinate the most common types of blade roots, appropriate critical root cross sections, shroud and damping designs in an order of increasing strength.

INTRODUCTION

Blade failures in steam turbines are not an uncommon occurrence. Concentrations of such failures are found with most major advancements, as a considerable increase in steam temperature, pressure, rotor speed, etc. One of such catastrophic failure series occurred during the 1930's. For a new line of topping turbines metallurgical improvements had made it possible to increase the steam inlet temperature from about 650°F to 900°F and the inlet pressure from 600 psi to 1250 psi. When these units came into operation, first row blades failed within 15 to 30 hours [1].

In comparing the design detail of some first row blade failures of the 1970's with those in [1], one finds that similar geometries and blade loading are still being used. Another

learning cycle might possibly be the reason for this. However, blade strength and cost are closely related and price comparisons of "upstream" versus "downstream" costs are difficult to be convincingly established.

There exist, of course, many different blade designs and most vendors offer an extensive variety of configurations for various levels of severity. The development of an understanding for the significance of these differences will be the purpose of the following discussion with a possible result for better judgement on the side of the user.

BLADE LIFE

Rarely is the longevity of a machinery part affected by so many parameters as that of a turbine blade. Contrary to compressor blading, turbine blades are subject to forces caused by higher operating temperatures combined with *transient temperature gradients* and the existence of higher *alternating blade loads* stemming from partial arc admission, wider wakes and flow mismatch due to extraction ports for steam and water removal, incorrect vacuum, etc.

Other factors affecting the longevity can be incurred during operation. Examples are: water induction, startup with bend rotor while blades are touching, operating at speeds of destructive resonant frequencies, incorrect steam conditions, steam impurities, etc.

A great influence on blade life, however, has the designer with the choice of mechanical and steam loading per blade, selection of shroud and root configuration for specific location in turbine, first row, intermediate, last row or transition region, stiffness of rotor root region, material selection, its hardness, manufacturing accuracy, surface finish, tightness of installation, etc.

From all parameters affecting the blade life, only those which relate to flow and strength of material questions will be considered.

1. Blade Forces

A most comprehensive presentation on the subject of blade loading and stresses is given in [2, 3]. For completeness and later referral, the forces acting on the blade are listed below:

- a) Centrifugal forces
- b) Centrifugal bending
- c) Steady steam bending
- d) Unsteady centrifugal forces due to lateral shaft vibration
- e) Alternating bending

Alternating bending includes forced and natural blade vibrations in the axial and circumferential direction, caused by unsteady steam forces, blade and blade package resonances and rotor torsional and axial vibrations. The latter two exciting forces remain generally unconsidered for blade designs; so

does the exciting force due to lateral shaft vibrations under (d). If shaft vibrations are present, the resulting alternating root stresses might further increase, depending on the phase relations.

Steady forces (a, b, and c) are rarely the cause for blade failures, unless a serious overload occurs as with a turbine runaway. Unsteady steam bending forces (e), however, are most frequently the primary cause for blade fatigue failures. Sources for the alternating forces are any type of flow disturbances, such as wakes, local cross flows, and shock wave phenomena. Contrary to axial flow compressors, the intensity of these disturbances is especially severe in steam turbines. Reasons are high pressure ratios per stage and high velocities (supersonic at times). Some examples are discussed below.

1.1 Partial Arc Admission

For turbine load control purposes the first impulse stage might receive steam only through a certain arc portion of the whole circumference. Several valves control the steam flow for a number of such openings. Each opening contains several nozzles. For further detail consider [1] and [4]. In Figure 1 for

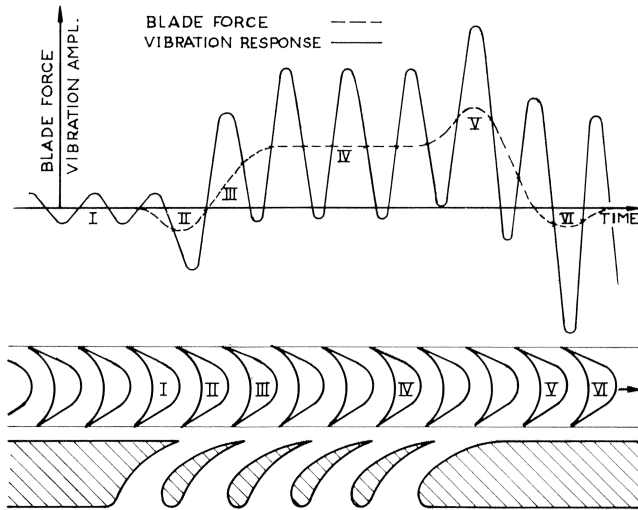


Figure 1. Blade Bending Force and Blade Tip Vibrational Amplitude of First Row Vanes Passing Through a Partial Arc [1].

a partial arc with several nozzles, the resulting rotor blade bending force and a vibrational blade response are shown. The vibration occurred here predominantly in the circumferential direction. Note that the negative force at the arc entrance and exit increase the total alternating force amplitude considerably.

The exposure of blades to the partial arc jets is probably the strongest fatigue mechanism in a turbine.

For many turbines the steam velocity, leaving the first nozzle row, is supersonic and complex shock wave interactions are known to aggravate the situation [6].

1.2 Wake Interaction

The effect of rotor blades passing in and out of a partial arc jet occurs in a milder form as blades pass through the wakes of a preceding blade row, as shown in Figures 2 and 3. Due to the momentum loss of flow near a blade surface, jets are formed, as the flow leaves the blade row. Intermixing of low and high energy flows might generate a velocity profile as shown in Figure 2. Figure 3 demonstrates the effect on the following rotor blade row. Noting that u represents the circumferential velocity, and c the alternating absolute velocity, the changing incidence of the relative velocity vector w becomes apparent. The effect on a blade is similar to that of a hand moving over a wash board. A detailed analysis of blade force fluctuations due to wake interference is given in [5].

The influence of a wake on the alternating bending force of downstream blades changes with the width of the wake. Less expensive or incorrectly designed nozzles, causing major flow separations and thus much wider wakes, will also cause higher force fluctuations.

Wider wakes downstream of well designed nozzles, on the other hand, can be due to an incorrect flow incidence or coarse turbulence in front of a nozzle row. An example for this is the flow between a control or Curtis stage (with partial arc admission) and the following stage (with full arc admission). A major step resulting from different mean diameters of the two stages may induce an additional secondary flow with the two 90° turns in the flow channel as shown in Figure 4, which can lead to strong flow separations, and a stimulus for both downstream stator and rotor blade row.

A similar effect on the force fluctuations, as that of wakes on downstream blade rows, can be generated by a downstream blade row or strut on an upstream blade row. As trailing edges move through the stagnation zones of downstream blades or

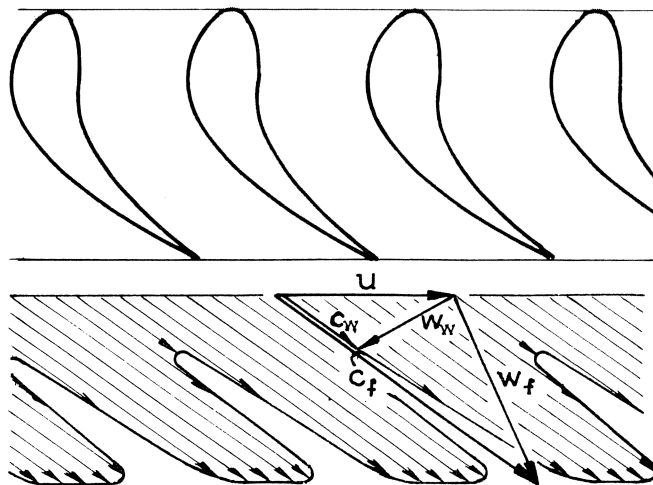


Figure 2. Velocity Profile Downstream of Stator Blade Row [5].

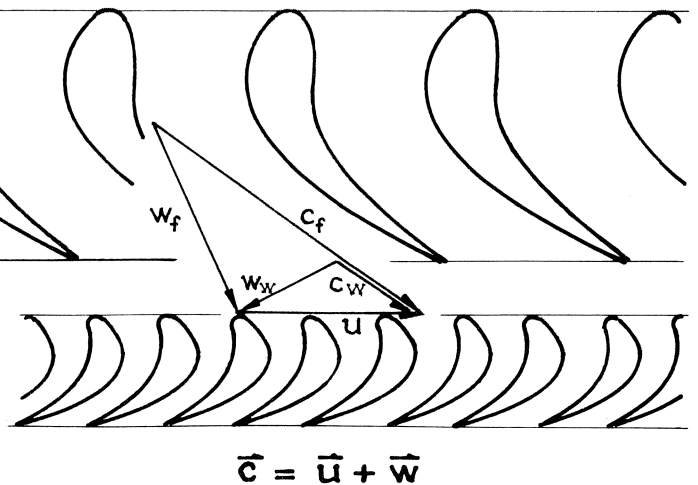


Figure 3. Changing Flow Incidence Caused by Wakes.

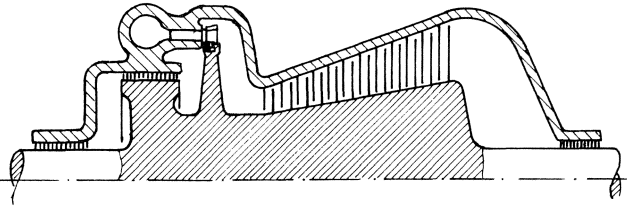


Figure 4. Region of High Turbulence Between Control Stage and Second Stage.

struts, a pulse is experienced. This is caused by a region of increasing pressure toward the stagnation point of a blade or strut.

1.3 Improper Flow Direction

Various sources can cause improper flow directions with respect to the leading edges of blades. Previously the incorrect incidence, as blades pass through the wakes of an upstream blade row, was discussed. An even stronger failure mechanism results if blades pass through flow fields with an improper direction of full speed flow once or several times per revolution. Examples for this are: differences in blade spacing (occurs mostly at horizontal joint of diaphragms), missing blade over locking port on rotor, improper match of nozzle sections at horizontal split [2], or even missing trailing edge section and any type of cross flows or eddies caused by steam extraction or water removal ports. The effect of improper blade spacing, missing trailing edge or missing rotor blade is shown in Figure 5. Local cross flows due to steam extraction ports, etc. might have a similar effect and are often a source of blade failures in adjacent rows.

To sustain the loading of steady forces, the blade strength can be determined quite readily. The danger for fatigue failures, however, lies with the above cited stimuli. The intensity of these unsteady forces, their frequency, magnitude and direction can often not be reliably predicted. This should be a major incentive for modifying the shape of certain blade root geometries to achieve lower magnitudes of stress concentrations.

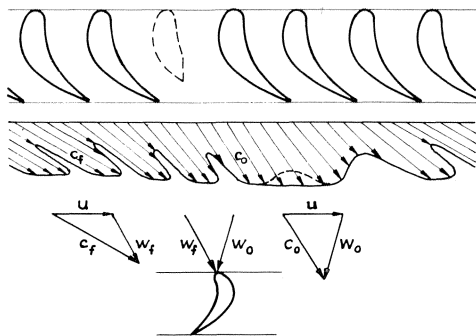


Figure 5. Change in Flow Direction Due to Missing Blade or Lost Trailing Edge at Horizontal Split.

2. Blade Fastenings

The majority of today's steam and gas turbines contain rotor blades, which are held in place by some type of root lands or serrations. Only in isolated cases and for some series of small units do we find blading which is an integral part of the rotor through either welding, hard soldering, electrochemical machining (ECM) or by casting. Blades, which are integral

with the rotor, have considerable strength advantages in comparison with blades held by root serrations, Figure 6 a, b, c, and d. A major disadvantage, however, is the difficulty and unreliability of replacing one or several blades, if damaged. Usually the whole blade row requires replacement. For electrochemically machined blades a replacement might be achieved with later introduced axial entry roots.

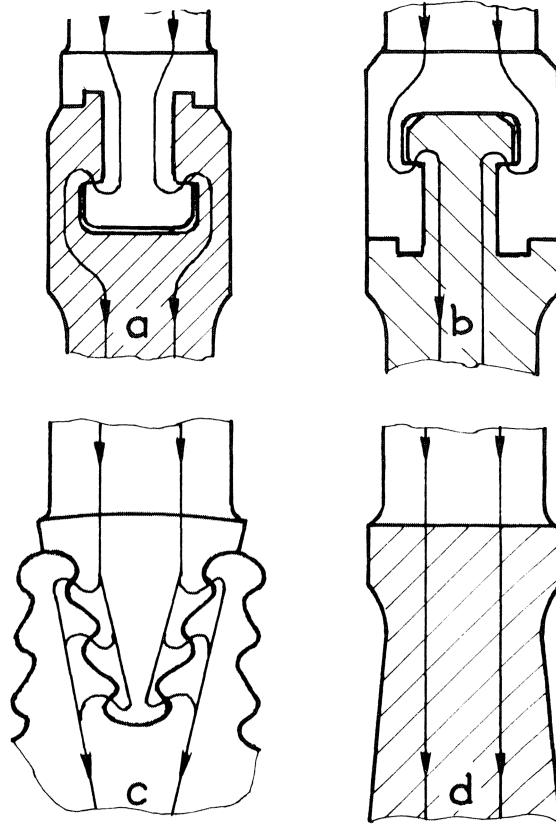


Figure 6. Load Transfer for Various Roots. a) Circumferential Internal Groove, b) Straddled Root [3]. c) Axial Sawtooth Root, and d) Blade Integral With Rotor [7].

Some of the basic shapes of blade fastenings are shown in Figure 7. The three columns A, B, and C represent circumferential type roots, the internal groove A, the straddled root B and the slotted and pinned root C. Column D shows axial entry roots and some of the integral designs.

3. Blade Root Geometry and Load Transfer

The most common types of blade fastenings in steam turbines were shown in Figure 7 under columns A and B. Blades, fastened in this manner, have to conform in their root design with the cylindrical geometry of the rotor.

For clarity of discussion the following planes are defined in Figure 8. Axial planes are formed by the centerline of the rotor and a radial line (these planes are perpendicular to the paper), radial planes coincide with the plane of the paper and circumferential planes are cylindrical surfaces as shown.

The two features, which a blade root should possess to conform with the cylindrical geometry, are a wedge shape, formed by the two axial planes and arc shapes for all circumferential surfaces, as shown in Figure 8. Any nonconformity will generate looseness associated with increased alternating stress

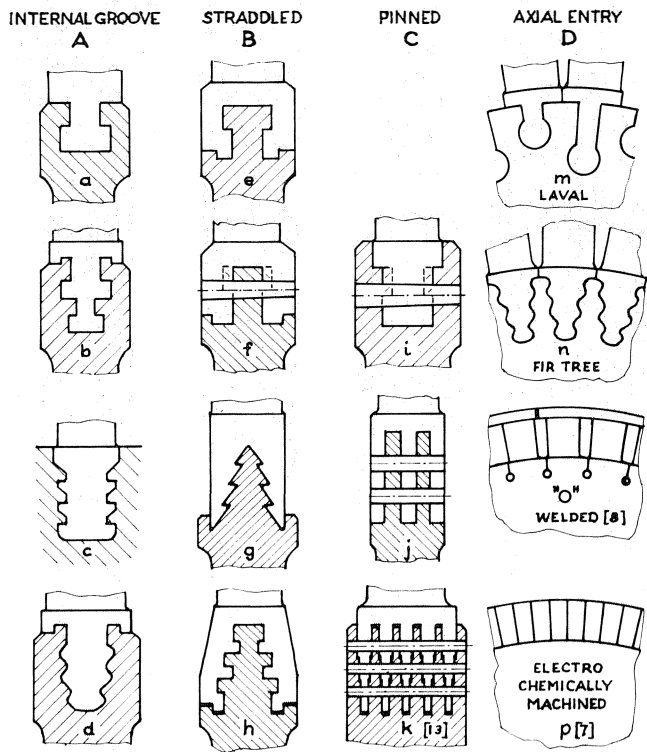


Figure 7. Blade Fastenings.

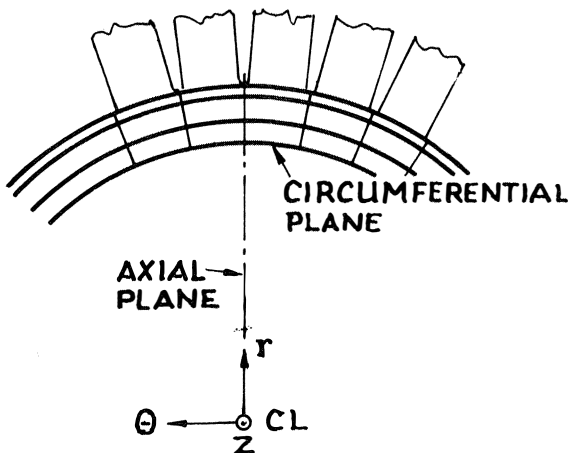


Figure 8. Conformity of Blade Roots With Cylindrical Geometry.

amplitudes and high concentrated contact loads, see Figure 9. Less expensive blades do not have curved root lands.

As difficult a task as it may be to achieve conformity with the cylindrical geometry, high reliability requires extremely high precision ($\pm .0004''$). This poses substantial demands on the accuracy of machining and quality control.

For the purpose of discussing some basic principles of load transfer from the blade to the rotor, an impulse blade with a symmetrical T-root, as shown in Figure 10, shall be considered. The blade forces, mentioned previously, shall for this purpose be grouped into centrifugal forces (radial) and into axial and circumferential bending forces. For the consideration of stiffness effects of both the rotor (drum or disc) and the blade

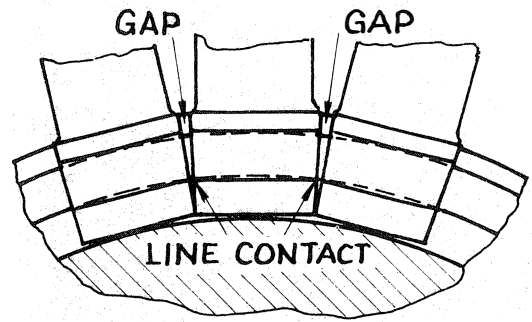


Figure 9. Blades not Conforming With Cylindrical Root Geometry.

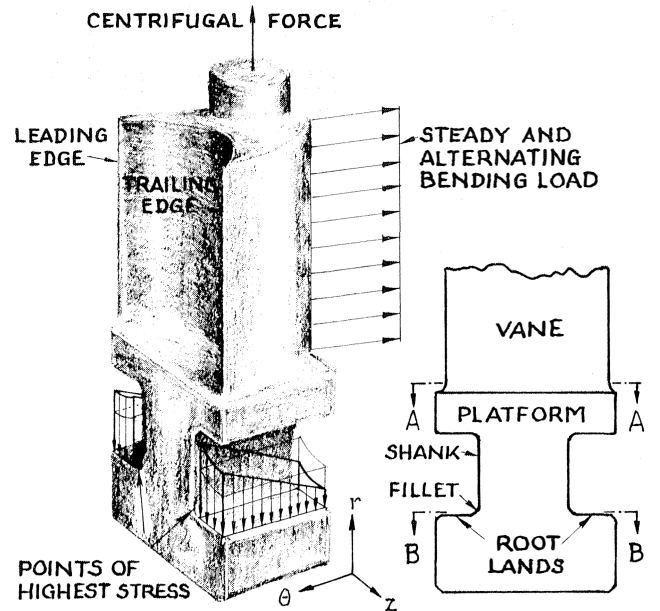


Figure 10. Load Distribution on Root Lands of an Impulse Blade.

root, the reduction of the bending force into its axial and circumferential component is required.

Starting with the pure bending moment, which is caused by the axial component of the blade force on the root, one finds that this moment is transferred right into the rotor, if the shank portion is tightly held by the rotor or disc, Figure 11a. In this case, the root lands are not required for the transmittal of this moment. If the root shank is not tightly installed, the moment will have to be transmitted by the root lands as shown in Figure 11b. In any event, for blades installed on a drum type rotor, the assembly is axially relatively stiff (high k value). For discs, the stiffness is smaller, especially if no retaining lips are provided, as shown in Figure 12. In such cases, disc fatigue failures due to axial force fluctuations can occur [2]. This is one reason why retaining lips are quite essential in disc applications.

The bending moment, which is induced by the circumferential component of the blade force, has a tendency to extract the blades from the rotor, similar to the action of the centrifugal force. The reason for this is the wedge shape of the blade as shown in Figure 13. The reaction forces, due to the applied moment, are perpendicular to the contact surfaces between blades. Their circumferential components form a moment and

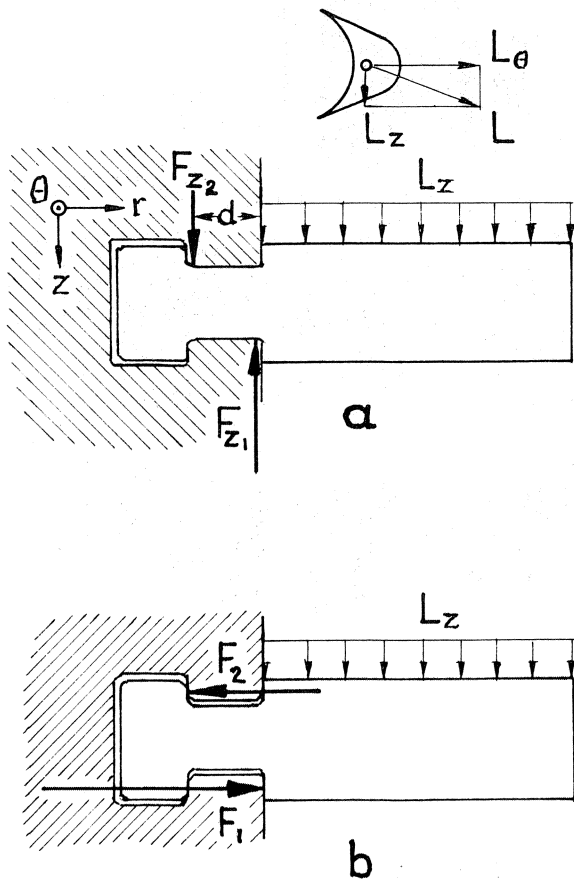


Figure 11. Reaction Forces Due to Axial Load for Cantilever Beam a) for Tight, b) for Loose Blade Shank.

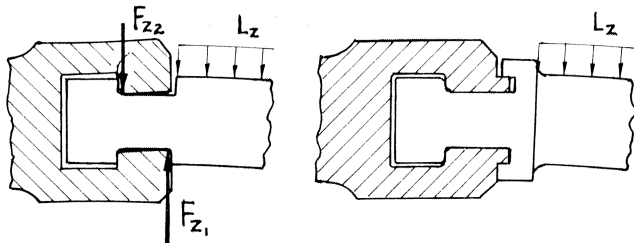


Figure 12. Disc Mounted Blade Without and With Retaining Lips.

a reaction force to balance the load. The radial components, however, are unbalanced, which require root lands. Depending on the angle of the wedge shape, the presence of the adjacent blades is more or less effective in transferring the bending moment into the rotor. In case of some looseness of the blade assembly, which can occur during transient conditions of the steam supply, it becomes evident, that the root lands may transmit a major part of the bending moment. Adding the resulting load distributions to that caused by the centrifugal force, a wedge shape load profile is obtained on the root lands, as shown in Figure 10.

In comparing the stiffness of the internal groove root assembly in the axial and circumferential direction, one finds that the assembly is considerably softer in the circumferential direction. This may explain why the circumferential component of the alternating bending forces is a predominant source

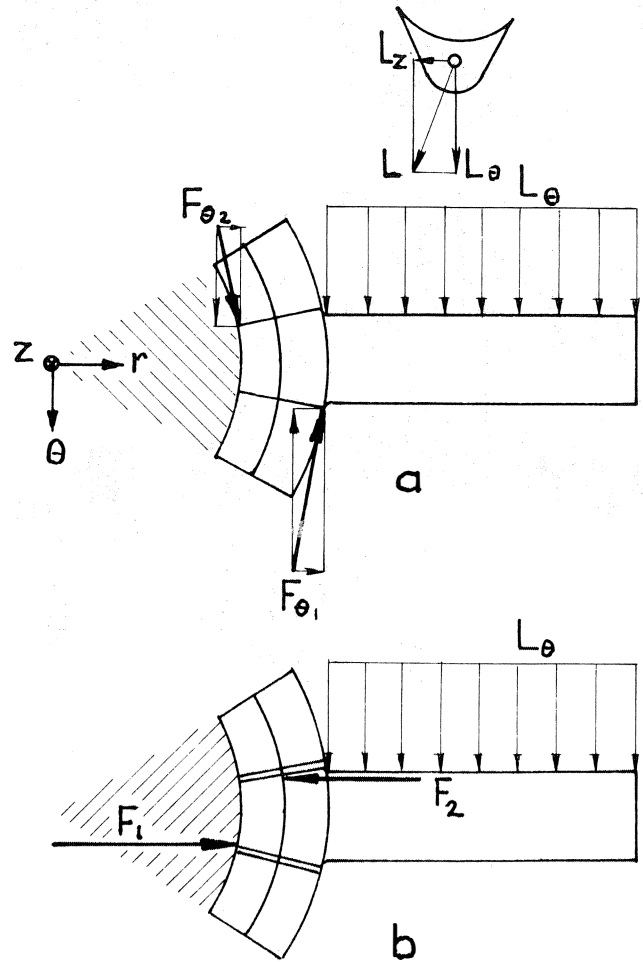


Figure 13. Reaction Forces Due to Circumferential Load for a) Tight, b) Loose Blade Assembly.

for fatigue failures of the internal groove root. The fact that for many vane shapes (reaction or impulse type) the circumferential component is equal or larger than the axial component, does not help this situation.

4. Stress Distributions in Blade Roots

Extensive studies of stress distributions in root cross sections have been performed by manufacturers and research groups. The photoelastic analysis technique is one of the common tools for obtaining information of stress distributions and stress concentrations. Figures 14 and 15 show the stress pattern in a T-root and more detailed in the vicinity of the fillet. One should note the very localized stress concentration just above the root lands in the fillet and shank portion.

Most photoelastic analyses concentrate on two-dimensional configurations, loaded by a radial force only [9]. The results reported in [10] correspond to such tests. Photoelastic measurements for the moment resulting from the axial blade force, similar to the case shown in Figure 11, could also be easily obtained. If considering the moment caused by the circumferential blade force on a simple T-root, the problem becomes three dimensional. Since the stress concentrations occur for this configuration in rather small regions, results are more difficult to produce. For more complicated shapes, the problem becomes even less translucent.



Figure 14. Stress Concentration in Fillet of T-root [3].

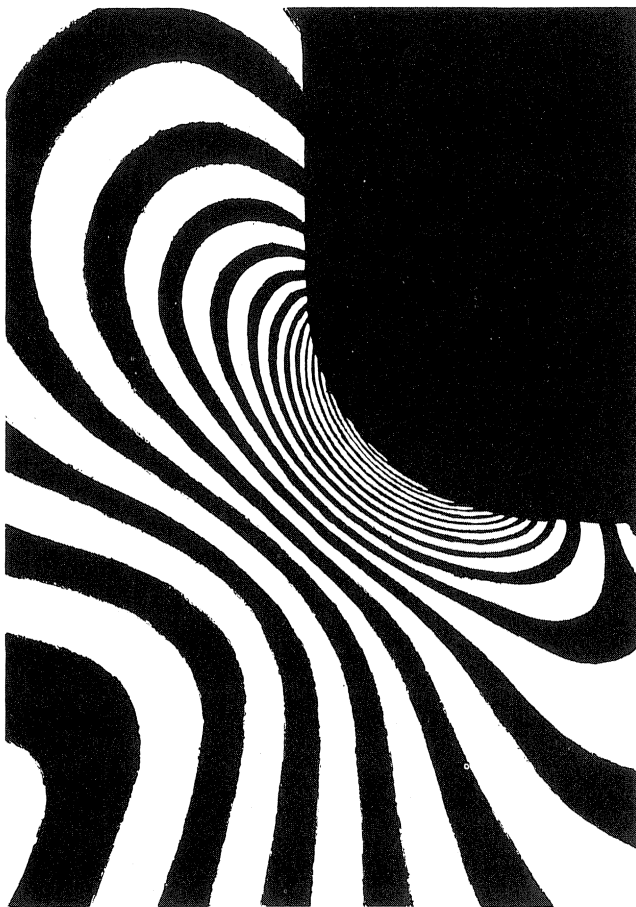


Figure 15. Close-up of T-root Stress Concentration [9].

For axial root cross sections (view of blade cross sections in columns A, B, and C of Figure 7), elaborate root geometries, subjected to tension only, have been studied and excellent optimizations have been achieved. As to the shape of circumferential root cross sections, for some designs the optimization appears to have been guided more by a desire for less expensive ways of blade manufacture or by trying to fit a vane shape conveniently to a root platform. Such shapes, however, do not necessarily become an optimum with regard to fatigue resistance against alternating bending stresses.

While finite element analysis is today a powerful tool for the design engineer, through its complexity the touch by means of simple thought processes for comparisons, especially in case of blade failure, might be lost. For this purpose an attempt is made to provide some insight into qualitative blade root stress distributions by considering circumferential root cross sections of various root designs.

As a method of identifying surface loading and stresses within a body in a qualitative manner, two types of cross-hatching symbols are used. As shown in Figure 16, a diagonal hatching shall represent tensile stresses, while parallel cross-hatching identifies compressive loading. The density or darkness of the hatching shall be a measure for the relative magnitude of either loading or stresses. The darker the area, the higher the stress value.

As a first example, a root cross section of an impulse blade with a T-root, as shown in Figure 10, shall be considered. The cross section is taken just above the top plane of the root lands as indicated. Figure 16 shows the load and stress distribution for a centrifugal load only. Due to flexing of the root lands the load increases slightly toward the shank. Stress concentrations

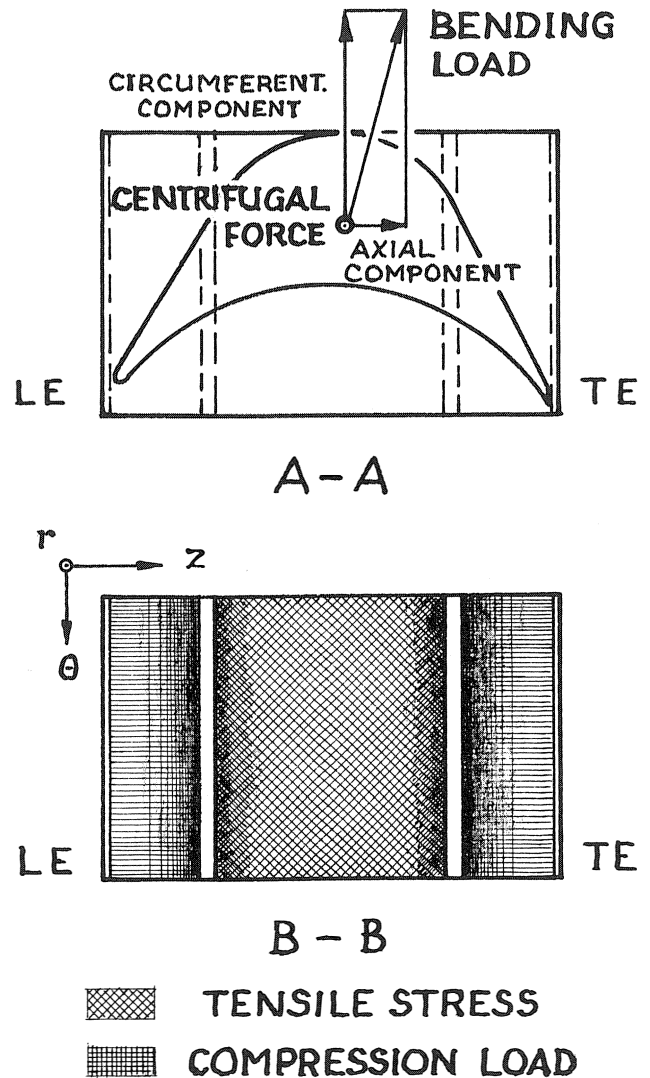


Figure 16. Load and Stress Distribution Due to Centrifugal Force Only. Ref. Fig. 10.

exist in the shank cross section on both sides near the root lands. This is in agreement with Figure 14, where the highest tensile stress occurs on both sides of the blade shank in the fillet region.

For the next two cases, the moments induced by the axial and circumferential blade force shall be added independently as a load to that induced by the centrifugal force.

Figure 17 shows the result of the superposition of radial and axial blade loads. If considering the more severe case of a loosely held blade shank, as shown in Figure 11b, the root land on the leading edge side of the blade would experience an increase in load, while the root land on the trailing edge side would experience an equivalent reduction. In a similar manner, the stresses in the shank will decrease from the leading to the trailing edge side. As mentioned earlier, the effect of a tightly installed blade shank would result in a lower stress concentration at the fillet on the leading edge side of blade. From the photoelastic stress analysis point of view, this configuration is still two-dimensional.

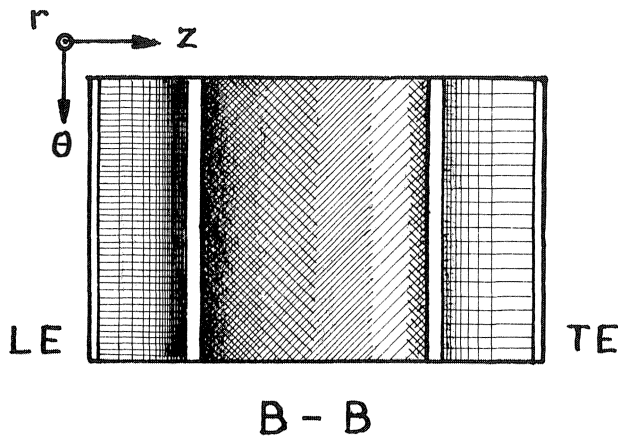


Figure 17. Load and Stress Distribution Due to Centrifugal and Axial Force. Ref. Fig. 10.

Figure 18 demonstrates the result of the superposition of radial and circumferential blade loads. Again, the more severe case of a loosely installed blade, as shown in Figure 13b, is considered. On the lands, the load has increased on the concave “pressure” side of the blade, while a reduction is seen on the convex “suction” side. Local high stress concentrations exist in both corners of the shank and the adjacent fillets on the pressure side of the blade. The stress distribution here is three-dimensional and a photoelastic analysis would require the method of stress freezing. For a blade, which is tightly locked in by adjacent blades, the stress in the corner may decrease. However, based on minute movements of blades relative to one another and a possible temporary or permanent looseness of the assembly, very high stress concentrations may result.

A superposition of the loading due to all three forces, radial, axial, and circumferential, would place the highest stress concentration in the fillet at the shank corner near the leading edge of the blade. In practice, however, for this type of blade and root shape, cracks seem to originate on both corners simultaneously. As will be seen later, for slightly asymmetric root cross sections of parallelogram shape, the failure starts most frequently on the shank corner near the trailing edge of the blade. This is a further indication, that the circumferential component of the blade force, together with a lower circum-

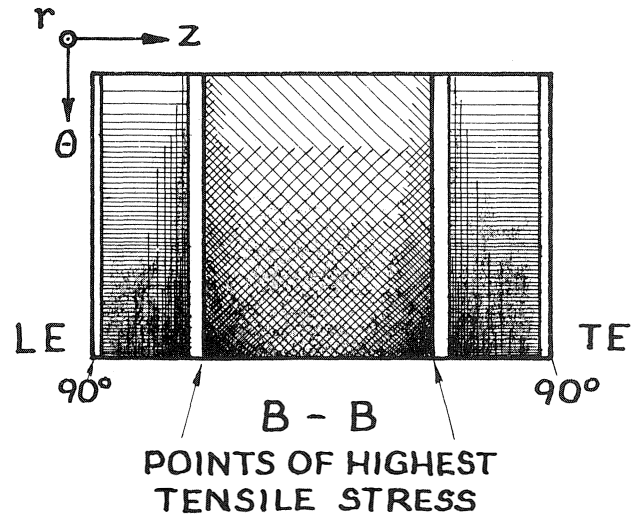


Figure 18. Load and Stress Distribution Due to Centrifugal and Circumferential Force. Ref. Fig. 10.

ferential stiffness, are more influential in inducing fatigue failures than the axial component.

The above example shows the detrimental effect of sharp corners on the root shank, especially in the presence of high alternating stresses. Well rounded corners at these locations are quite essential.

As can be seen from Figure 14, the severity of the stress concentration exists only in the shank cross section, just above the root lands. In accordance with Saint Venant’s Principle, the stress becomes more evenly distributed in a cross section slightly above. Here a stress distribution would have a similar appearance as that in Figure 19.

A reduction of the stress concentration in roots of this type can be obtained by adding a third load carrying surface, which joins both highly loaded edges, as shown in Figure 19. The additional root land will be held down by a notch provided by the adjacent blade. In this manner, the load spikes and the stress concentrations are removed as a result of better load distribution. This is achieved by transferring some of the load to the lighter loaded opposite side of the root of an adjacent blade. As a result, the stresses are also more evenly distributed over the whole cross section. In the past, the same idea has been used to secure locking pieces. A similar reduction of stress concentrations on existing units can be achieved by installing axial damper pins through root platforms between blades [2].

Asymmetrical impulse vanes and especially reaction blades are difficult to place on a symmetrical (rectangular) root platform, unless one leaves the trailing edge unsupported, or a cutout is provided, Figure 20. These vanes are conveniently mounted on root platforms of parallelogram shape. Still, depending on the chord to pitch ratio, in dealing with impulse vanes, both the leading and trailing edges might be overhanging. In Figure 21, the stress distribution of an impulse vane mounted on an asymmetrical platform is shown.

A parallelogram shape introduces two significant changes in root strength. First, in the previous case two high compressive edge contacts existed, which induced high stresses in the two 90° corner regions of the root shank. The new configuration indicates, that the highest compressive load is applied even more localized at the tip of one land. From there the highest stress is induced in the adjacent shank corner. The

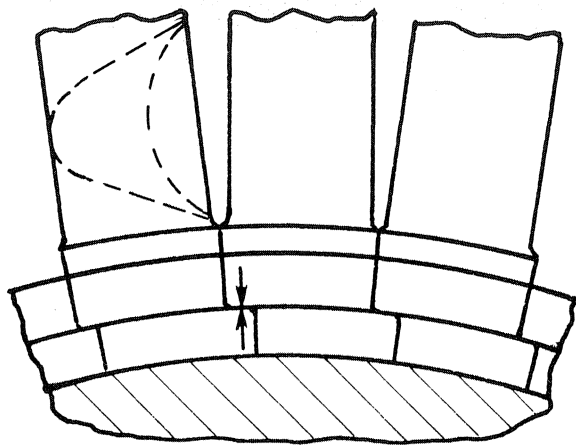
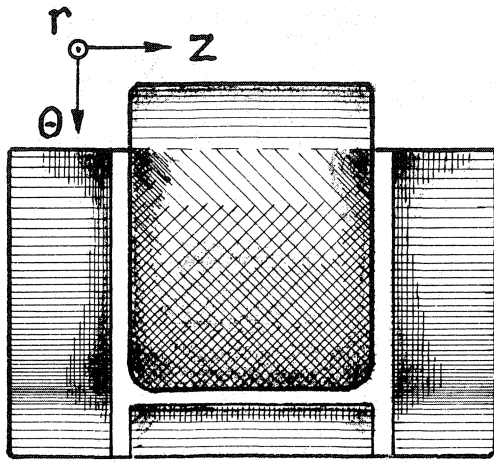


Figure 19. T-root With Reduced Stress Concentrations.

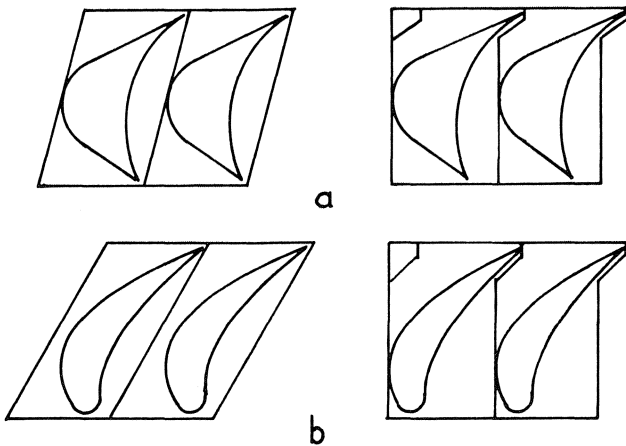


Figure 20. Vanes Mounted on Parallelogram and Rectangular Shaped Root Platforms, a) Impulse, b) Reaction Blade.

angle of this corner is less than 90° . This, in turn, causes a higher stress concentration than in the previous case.

Secondly, for the previous configuration the highest compressive loads were induced on the edges of two struts with an outer angle of 90° . This results in a stiffer (higher k) assembly.

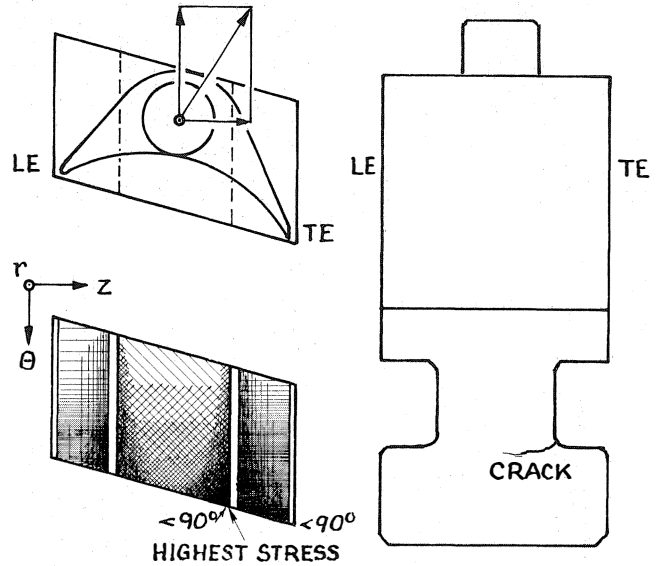


Figure 21. Load and Stress Distribution for Parallelogram Plate Mounted Impulse Blade with T-root.

For the parallelogram root, however, the highest compressive stress is induced at the tip of a single land with an outer angle of less than 90° . This configuration will cause a softer (lower k) assembly.

With a further decreasing shank corner angle, the stress concentration becomes more severe and the stiffness k of the land corner decreases further. The amplification effect of alternating stresses, due to the low k value, is a well known phenomenon.

From the preceding discussion it can be concluded, that the strongest configuration for the internal groove root is one with a rectangular root cross section. The diagrams also explain, why fillet cracks of the asymmetric root type originate on the trailing edge (TE) side of the root. This holds true for both, the impulse and reaction blading mounted on parallelogram shaped root platforms. Even for minor deviations from a rectangular shape (-2°) failures are experienced more on the trailing edge side. This is rather surprising if one considers the direction of the total bending moment.

In parts made of ductile material, which are predominately subjected to steady stresses, high stress concentration may not be a cause of failure. Through small amounts of yielding, the stress field can adjust itself. In a situation, however, where high alternating stresses persist, as in the case of rotating blades, high stress concentrations should be avoided. Local overstressing, reversing yield, embrittlement and crack formation will lead to an eventual fatigue failure.

Using the above developed criteria, blades of various root geometries shall now be considered. For this purpose blades shall be classified in the following manner:

- a) Ultra heavy service or Ultra high strength
- b) Very heavy service or Very high strength
- c) Heavy service or High strength
- d) Medium service or Medium strength
- e) Light service or Low strength
- f) Very light service or Very low strength
- g) Ultra light service or Ultra low strength

It should be understood that these classifications apply only to

the geometrical shape of blade roots and shrouds. Based on differences in steam quality, operation, blade surface preparation, installation, location of blades within the unit, first row, intermediate rows, or last row etc., one type of blade may fail before another.

4.1 Internal Groove Root

The previously discussed T-root with rectangular or parallelogram shaped cross section, belongs to the internal groove type. Variations were shown in Figure 7 under column A. The internal groove root is very common in steam turbines and many stationary blades are fastened in this manner. A reason for the popularity is the relative ease of manufacturing. When used on rotors, the final locking piece often represents the weakest member and can be a source of problems.

4.1.1 Drawn Section Blades

Based on an old aerodynamic design theory for cascades, and the economy of manufacturing, early blades were made from thin sheet metal. These blades were separated at the root by spacer pieces, as seen in Figure 22. Note the sizable overlap of the spacer piece.

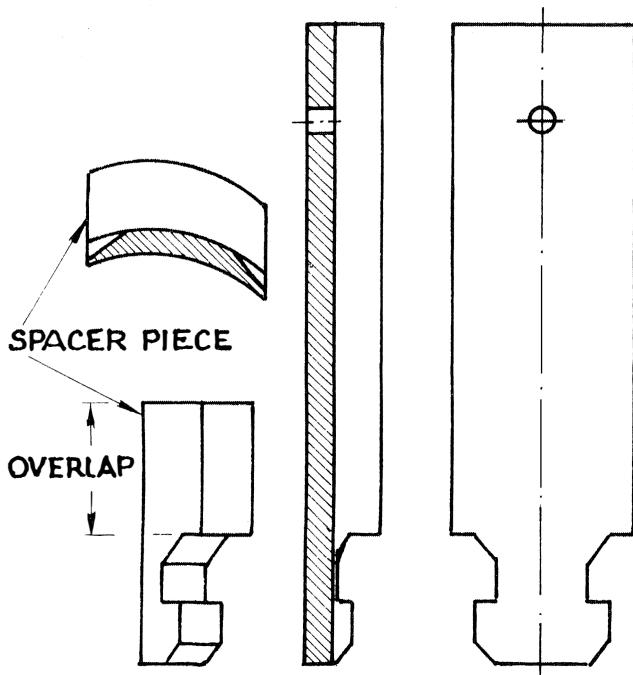


Figure 22. Sheet Metal Blade and Spacer Piece [15].

The same basic configuration is used today with drawn profiled steel blades. The two most common root shapes for this type of design are shown in Figure 23 a and b. These correspond to types A,a in Figure 7. The overlap, which was shown in Figure 22, is very often not provided. This results in a major contact force at the top of the shank, at the base of the airfoil. In addition, a high stress concentration exists at the sharp corner of the shank on the trailing edge side, as indicated. The angle there is less than 90°. Also the highest load is induced at the very soft tip of the root land. Spacer pieces are sometimes made out of powder metal, which allows the blade assembly to become loose with time. As mentioned, looseness amplifies alternating stresses.

This type of blade design is acceptable for stationary blade applications. If used at all as a rotating blade, it should only be

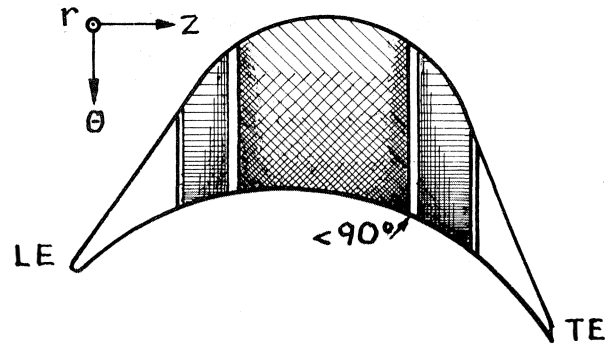
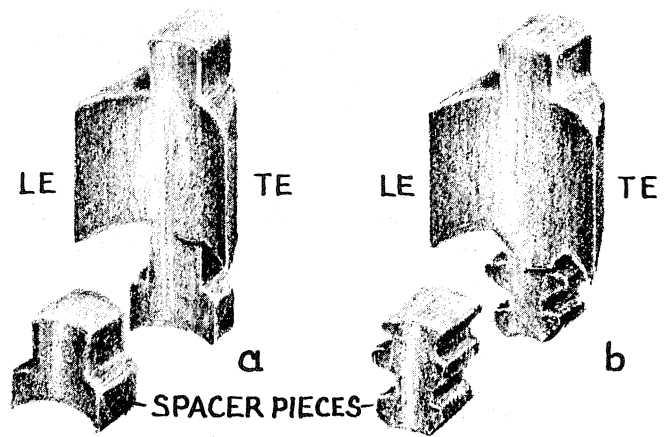


Figure 23. Drawn Profile Blades with Spacer Pieces a) T-root, b) Serrated Root.

considered for ultra light service, third or fourth stage. When used in a first stage with partial arc admission, the probability of a failure is very high. In addition, the price to replace all blading, in case of a failure of the first row and its consequential damage might outweigh the original purchase price for blades of the fully milled kind.

For the above design to graduate into the blade category for very light service, the following conditions should be met:

- Provide overlap for spacer pieces.
- Select bar stock material for spacer pieces, not powder metal.
- Provide for both, blades and spacer pieces curved contact surfaces to conform with the curvature of the circumferential groove.
- Provide retaining lips.

4.1.2 Bar Stock Blade

Fully milled blades are generally referred to as bar stock blades. The two examples, which were discussed previously and shown in Figures 10 and 21, belong into this group. The manufacturing cost for the fully milled type is substantially higher than for the drawn blades.

4.1.2.1 Curved Root Cross Section

The blade has the same shape as those shown in Figure 23a or b, with the spacer piece being an integral part of the blade. Its strength could be rated somewhere between the drawn section blade and the blade with asymmetrical T-root, discussed in the next section. Its main weakness is the addi-

tional stress, caused by centrifugal bending. As seen from Figure 24, the moment is created by discontinuities of the line joining all centers of gravity of all blade cross sections, from root to tip. The same problem existed with the drawn section blade. The weaknesses of the drawn section blade, shank corners less than 90° and the flexible root land tip, are also found here. The increased shank cross section (crosshatch area in Figure 24), improves its strength.

4.1.2.2 Single T-Root

If blades with a single T-root, Figure 10 and 21, are used on discs, retaining lips, as shown in Figure 7A,b and A,d, are important to prevent disc rim failures. Still, this blade would be suitable for light service only. For some small turbines (1000 to 2000 HP), these blades might be used in the first stage. An asymmetric root cross section should, however, be avoided. If fatigue failures in the root do occur, a series of remedial actions, such as strengthening the shroud, adding lashing wires, etc. can be suggested. Another possibility would be to use a horseshoe shaped root land, as shown in Figure 19. In any event, a thorough investigation should be conducted.

4.1.2.3 Double T-Root, Serrated Root

For more demanding applications double T-roots or serrated roots, as shown in Figure 7A,b or A,c and d, are used. If these blades are installed on discs, retaining lips are mandatory. The reason is a much stronger crowbar effect of the longer blade root and the more flexible disc rims, caused by a deeper groove, as shown in Figure 25.

As mentioned previously, impulse or reaction blades utilize predominately parallelogram shaped root platforms. With applications ranging between medium and high strength service, these blades with serrated or double T-roots are still quite vulnerable to fatigue failures. Considering Figure 26, a load profile has been indicated on the first serration. A similar

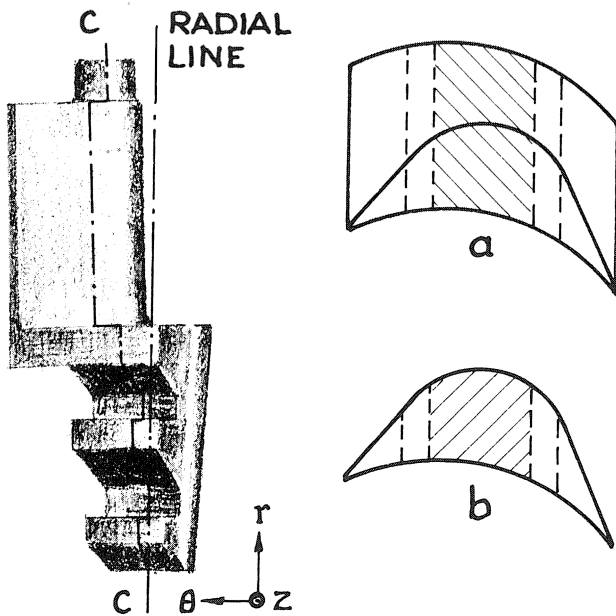


Figure 24. Milled Blade with Centrifugal Bending. Note the Deviation of Line C, Joining Centers of Gravity of Cross Sectional Areas, from Radial Line, or Unsupported Overhanging Mass. Cross Hatched Areas show Bigger Shank Cross Sections for Milled Blade a) than Drawn Blade b).

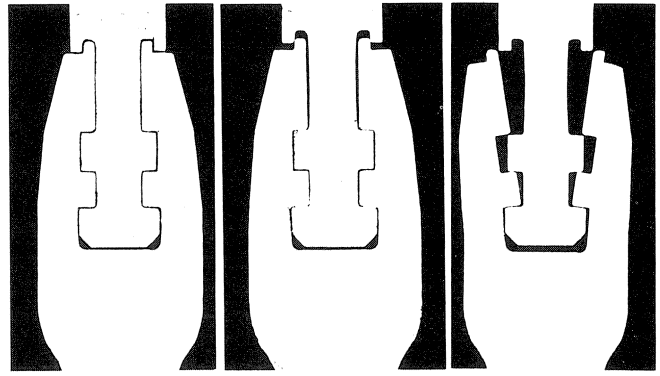


Figure 25. Tension Test of Double T-root Showing Effectiveness of Retaining Lips [3].

profile would be located on the serration below. The highest load spike, which occurs on the top serration near the trailing edge, is responsible for inducing fatigue cracks in the adjacent fillet and shank corner region as shown. Changes such as further rounding of the shank corner or undercutting the tip of the serration might help, but these do not remove the inherent stress concentration. For a given rotor root geometry, a remedial action would be to provide blades with a rectangular root cross section, with an overhanging, but supporting trailing edge. This feature was mentioned in Section 4 and will be shown in Section 5.2. Preloading each blade with a key at the bottom of the root, would be a further substantial improvement. This will be discussed in Section 4.6. Other remedial actions are described in [2]. The load and stress distribution presented in Figure 21 is comparable with that, which could be drawn for this case.

4.2 Straddled Root

An inversion of the internal groove root forms the straddled root. Some of the more common configurations are shown in Figure 7 under column B. Because of its geometry, this root is used solely on discs. A rating of this blade root may place it in the medium to heavy strength category. The straddled root has some advantages over the internal root [3]. These are, first, an overall light root-disc rim weight, see Figure 27 a and b, and secondly, a larger area moment of inertia of the root shank cross section about the principal axis in the circumferential direction. The moment of inertia about the axial principal direction, however, is unchanged. This is demonstrated in Figure 27 for a symmetrical T-root of the type A,a and the inverted, straddled root of type B,e.

The larger area moment of inertia about the circumferential axis may cause a slight decrease in the magnitude of stress concentrations, due to the axial blade force. This however, is generally the smaller of the two components, which is less responsible for blade root fatigue failures. The stress concentration, caused by the circumferential blade force, remains essentially the same.

Most of the straddled root designs utilize a rectangular vane platform. In this case, this is also the optimum shape for minimum stress concentrations. Generously rounded off shank corners help to further reduce stress concentrations. The size of the radius should be the same, as the fillet radius. A typical load and stress distribution is shown in Figure 28a.

For a parallelogram shaped vane platform the stress concentration increases on the trailing edge side with a decreasing corner angle in a less severe manner as for the internal groove

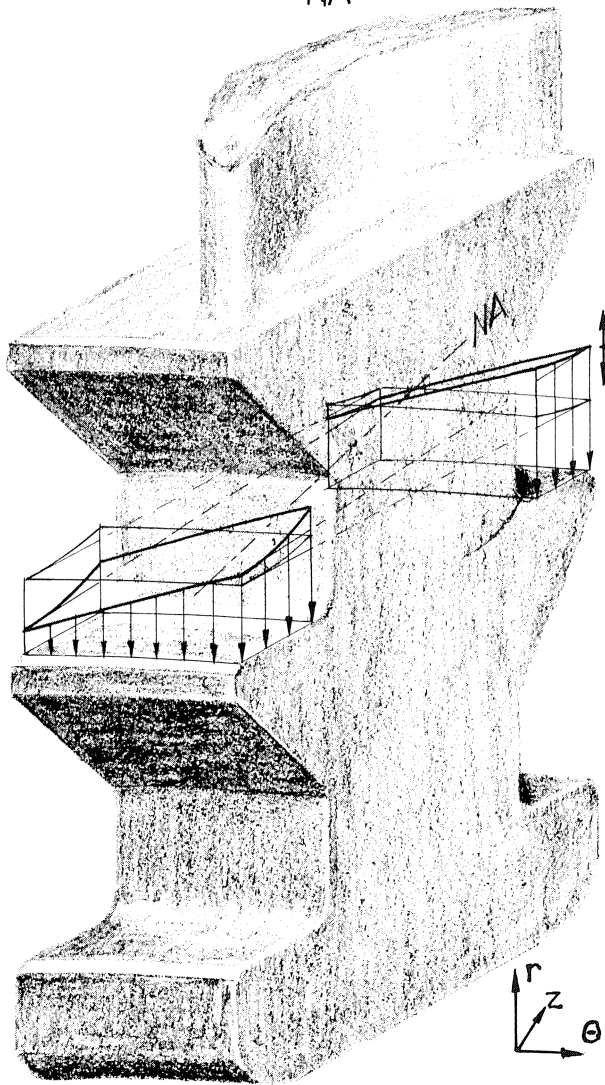
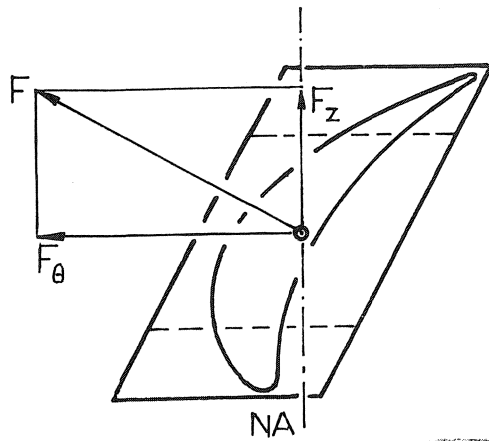


Figure 26. Load Distribution on Serrated Root, Due to Radial and Circumferential Forces.

root, Figure 28b. Here, the critical angle becomes greater than 90° . This causes less localized stress concentrations and an overall better stress distribution as in the case of the internal groove root.

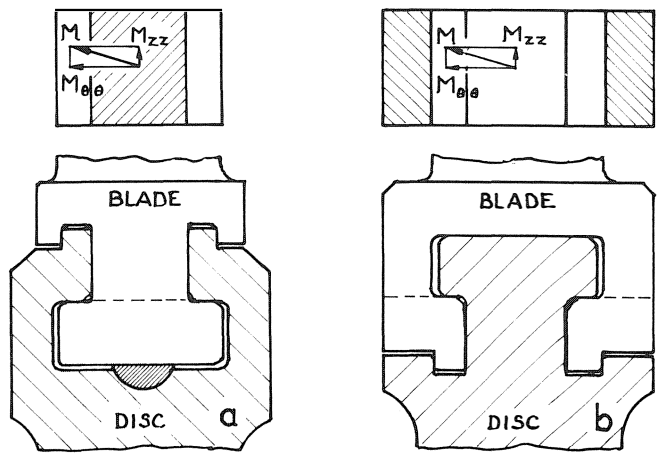


Figure 27. Comparison of Area Moment of Inertias for a) Internal, b) Straddled Root.

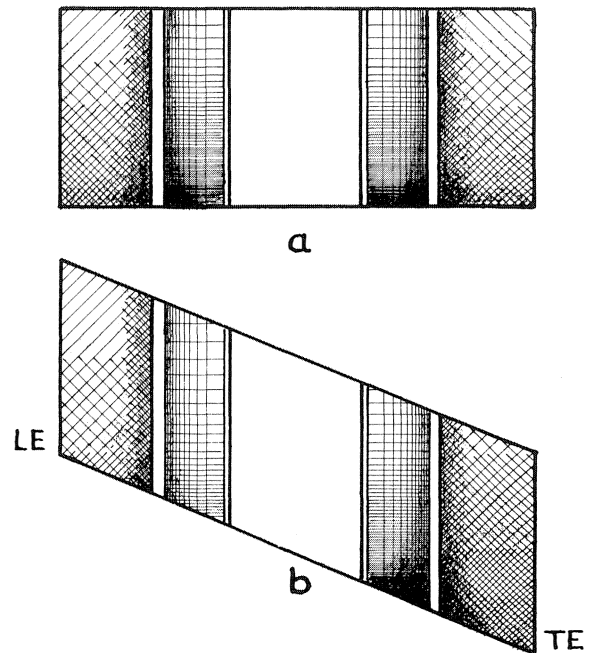


Figure 28. Load and Stress Distribution for Straddled Roots of a) Rectangular, b) Parallelogram Cross Section.

4.3 Grooved and Pinned Root

Many of the locking devices used for the internal groove root and the straddled root are pinned or riveted to the rotor, Figure 7, column C. Since those devices (often a single blade with a special root shank), are the most highly loaded members in blade rows, the use of pinning is generally considered quite reliable. Problems can arise, if a locking piece, held with one or two rivets, has to absorb a portion of the circumferential blade force of the whole blade row of a highly loaded stage. The magnitude of this portion cannot be defined reliably. Pin failures have occurred in those cases. However, if every blade in a row is pinned or better, if the pins are inserted between blades in a staggered manner, as shown in Figure 29, the strength of the assembly can be compared with that of an axial entry root. This is the case, except for a higher weight of the

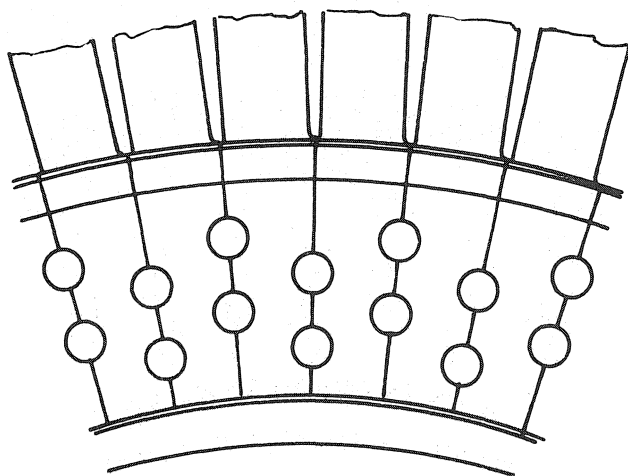


Figure 29. Sideview of Blades Pinned to Disc [3].

root combined with the disc rim [3]. A rating would classify it as of very high strength.

Some manufacturers use this fastening technique for last stage blades. Locking devices are not required with this design.

The replacement blades for the 1930 disaster, mentioned in the introduction, was of a configuration shown in Figure 30. Three blades are welded together and pinned as a package to the disc.

4.4 Axial Entry Root

Column D of Figure 7 shows two axial entry roots, the Laval type and the fir-tree root. Today the Laval type is mainly used for axial compressor blades, whereby the bottom half of the cylinder is not provided. For steam turbines it is only used

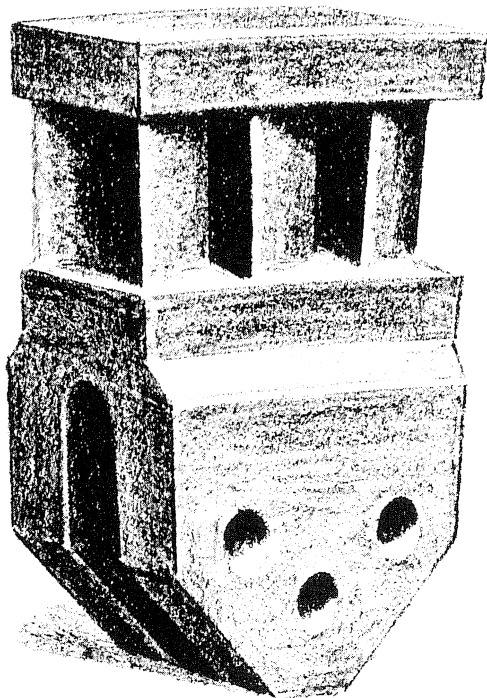


Figure 30. Three Blades Welded Together Form a First Stage Blade Package [1].

in few cases, because of its apparent weakness in the root cross section, just below the vane platform [3].

By today's standards, the axial entry fir-tree root receives the highest rating of ultra high strength. This is why many steam turbine manufacturers use it for the first and last stage, and many gasturbine manufacturers provide it for all stages. Through many excellent features it has established itself as the most superior design of all nonintegral blades. Figure 31 shows an example of a first stage blade. The sketch of load and stress distributions above the first root lands from the top, does not show any stress concentration. Slightly higher stresses exist in the root shank on the suction side of the blade. But all stresses are of nominal value, even at critical corner points. All root lands can be machined straight, except for some last stage blades, where the root is curved to achieve a required high hub solidity. With regard to alternating circumferential blade forces, the root displays excellent damping characteristics. Even loosely inserted blades (used mainly in gasturbines) have the tendency to tighten up against the wheel flanks with increasing rotor speed. This is not found with any other root design. Root fatigue failures are very rare and may occur only if either shrouds or lashing have failed prior. A further positive feature related to thermal expansion is discussed in the following section.

To reduce the slightly higher stresses in the shank on the suction side of the blade may suggest that a parallelogram shape of the root cross section would be the optimum choice. The shape would be such that the total blade load vector is perpendicular to the long sides of the parallelogram, as shown in Figure 32. While the stresses in the root may be lowered with the corner angle of the shank, becoming larger than 90° , for the rotor, however, the stress concentration in the adjacent shank corner with an angle of less than 90° , would increase. For this geometry, rotor failures have occurred. One could therefore state that for the axial entry root, the rectangular cross section is an optimum choice.

No highly loaded locking device is required with this design. Some examples are shown in Section 4.7.

4.5 Unsteady Temperature Gradients

During startup the blading can become for short durations substantially hotter than the rotor. This occurs especially in the high pressure region of turbines. High compressive stresses in the blade roots, outer rotor layers and the shrouds can result, Figure 33. Gaps between shroud segments make allowance for the expansion and the resulting stresses are therefore minimized. Provisions to reduce these stresses in the outer rotor layers are not present with most blade root geometries, except with the axial entry sawtooth root, as shown in Figure 34. This is another feature, which lets the axial entry root be a superior choice for high temperature service (900°F and higher).

As long as the expansions stay within the elastic range, designs, utilizing the internal groove root or the straddled root, may not experience a loosening of the blade assembly. However, with high temperature units and high stage loading, such overstressing may cause a plastic deformation of the blade root assembly, resulting in looseness. This gives rise to an amplification of the circumferential component of the alternating blade force.

4.6 Positioning and Preloading of Blades

Axial entry blades stand out with their advantages of self-tightening, vibration dampening, and the ability to absorb differential thermal growth. The internal groove and the strad-

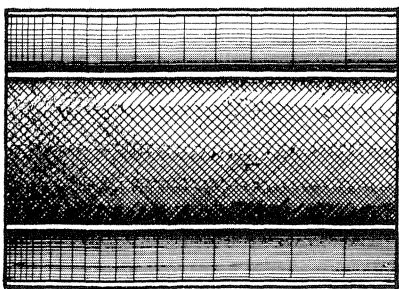
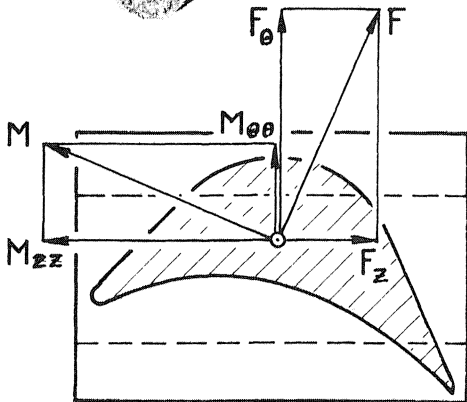
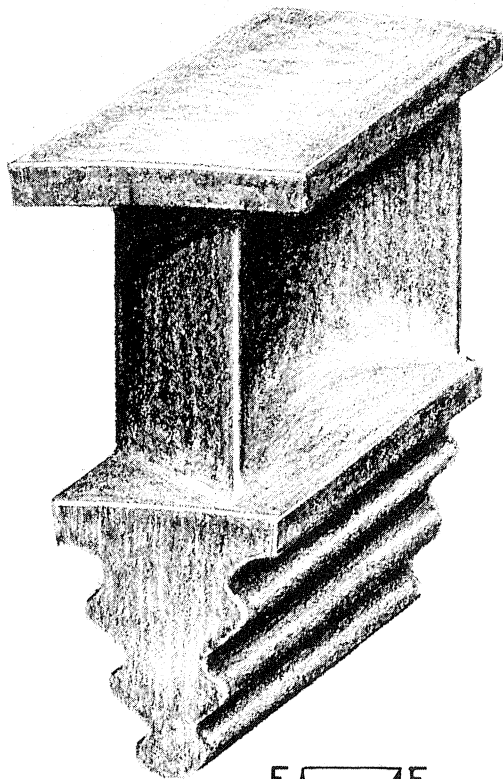


Figure 31. Load and Stress Distribution for Axial Entry Blade.

dled root, however, lack these features. Instead, when both blade types are being assembled, a tight contact of blade root lands and rotor lands has not been achieved, mainly due to necessary tolerance provisions. This is noted during a first runup and overspeed test. Often a rotor requires even a balance correction after "the blades have set". During the runup, the blades readjust from their as-installed position to a

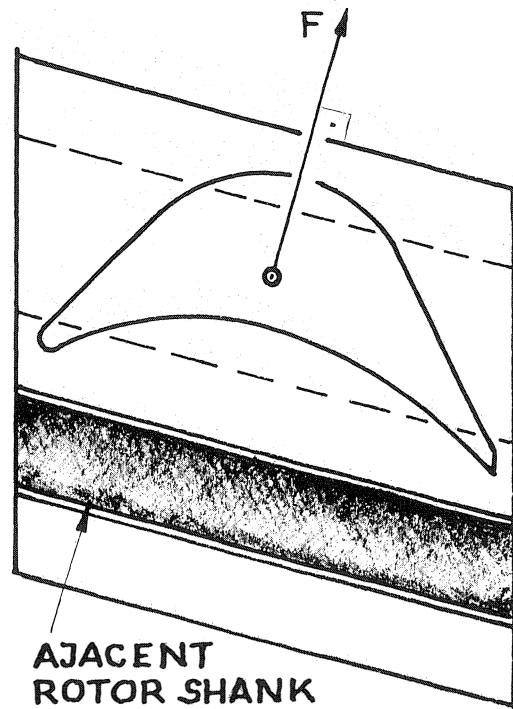


Figure 32. Blade Bending Force Perpendicular to Root Lands Causes Stress Concentration in Adjacent Rotor Shank.

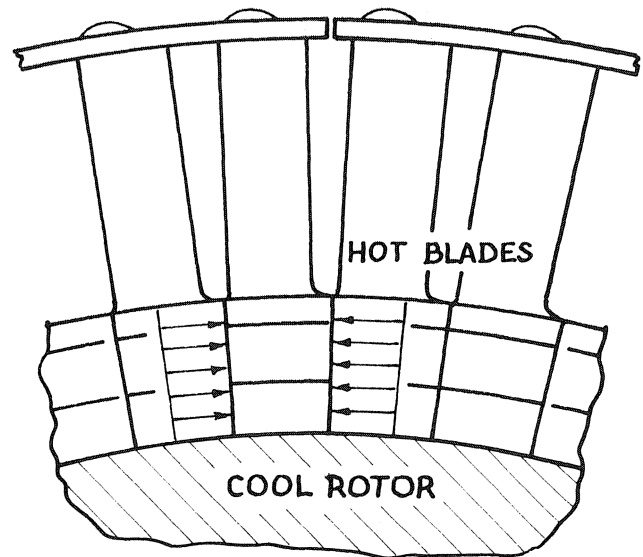


Figure 33. Circumferential Crush on Roots, Due to Temperature Difference Between Rotor and Blades.

new operating position, which generally is slightly further outward. This may certainly be accompanied by some localized yielding. Because of the wedge shape described in Section 3 a slight radial blade displacement may introduce some looseness, even before the unit goes into operation.

To overcome the readjustment of blades, some manufacturers have installed single or multiple keys for blade positioning, as shown in Figure 27a. This has several merits. It provides a tight contact between seating surfaces of blade and rotor, the blades can be fitted much tighter against one another

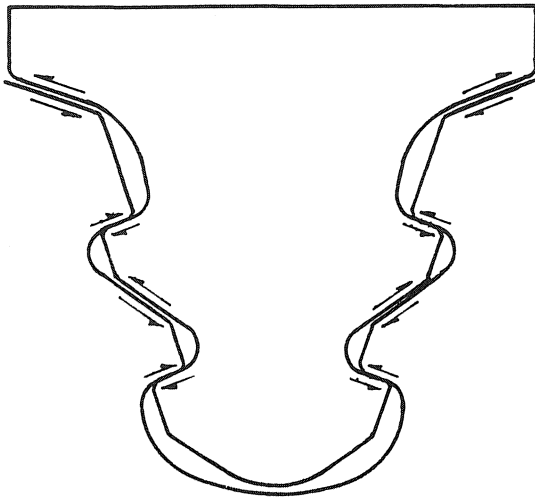


Figure 34. Capability of Root Expansion on Case of Temperature Differential Between Blade and Rotor for Axial Entry Root.

and a reduction of the amplitude of the alternating stresses in the blades will result due to the preloading. Because of the difficulty of assessing these advantages qualitatively, and due to the additional work, only few manufacturers are using this procedure today.

Another form of preloading is to induce compressive stresses in the outer blade root layers by means of shotpeening. High spikes of tensile stresses, which were seen to occur in certain blade regions near the surface, are hereby reduced to some degree.

4.7 Blade Locks

The internal groove and straddled root designs generally require an entrance port, where all blades for a particular row are inserted and slid into their final position. At this location the rotor serrations have been milled away, allowing a blade to be "threaded", as a pearl on a string, as shown in Figure 35. In Figure 7f and i, it is indicated how a locking device for the straddled and internal root could be shaped respectively. The dashed lines indicate the original contour. The existence of the

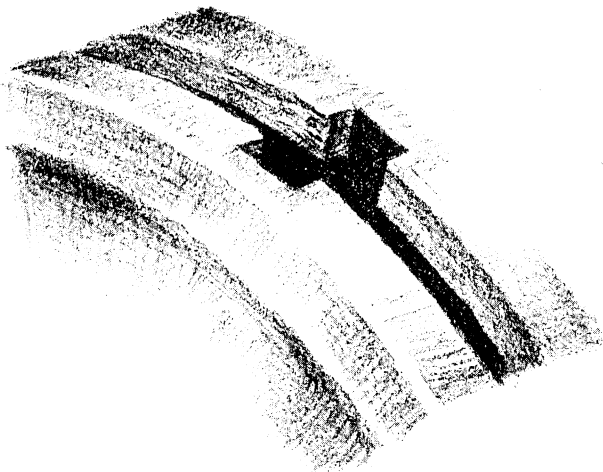


Figure 35. Entrance Port for Blade with Internal Root.

discontinuity in the rotor serrations makes the weakness of this region quite apparent.

Generally the locking pieces or the last "locking blade" are the highest stressed members in a blade row. Avoiding the weight of a "last blade", by simply installing a much lighter spacer into the entrance port, helps to reduce highly stressed parts, but introduces a strong fatigue stimulus as discussed earlier.

With the internal groove root design there exists one exception, which does not require an entrance port. In this case, the blade shape allows each blade to be inserted and twisted less than 90° into position. Thin spacer pieces between the last few blades make up for the required width for one blade and are inserted in pieces, as shown in Figure 36. Other intricate methods have been used in the past [3, 11].

Axial entry blades require minimal fixation. Some examples are shown in Figure 37. The good reliability of these relatively weak axial blade fixations are a further proof of how little effect the axial bending force has on the fatigue of this fixation or the blade root, even for the axial entry geometry.

5. Vibration Damping

Strong blade excitation forces in steam turbines require the use of vibration damping in many stages. For reliable operation through a wide speed range, most types of industrial turbines employ either shrouds or lashing in all stages. The constant operating speed of generator drivers allows the omission of damping devices for intermediate stages and, in rare cases, even for last stages. For larger units, 200 MW and up, damping is found almost exclusively with all stages. In selected cases free standing last stage blades, stiffened by centrifugal bending, have been quite successful.

5.1 Shrouding

By comparing a cantilever beam with a free standing blade, a beam supported at both ends would correspond to a blade with a fixation at the root and the tip. The blade fixation (shroud) at the tip is a metal strip. It is wide enough to cover the blades axially and is fastened by riveting, welding, etc. to

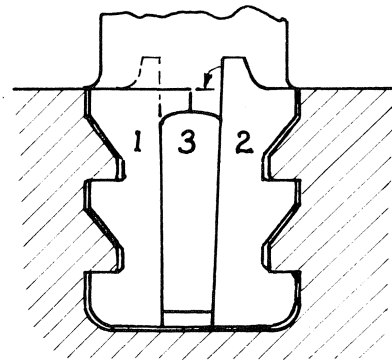
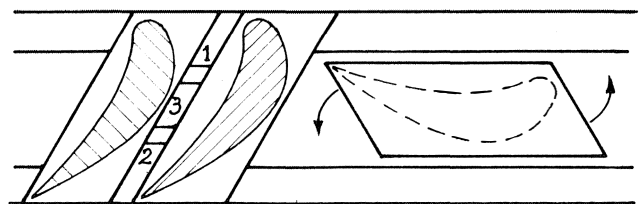


Figure 36. Blade Lock Without Locking Port Hole [3].

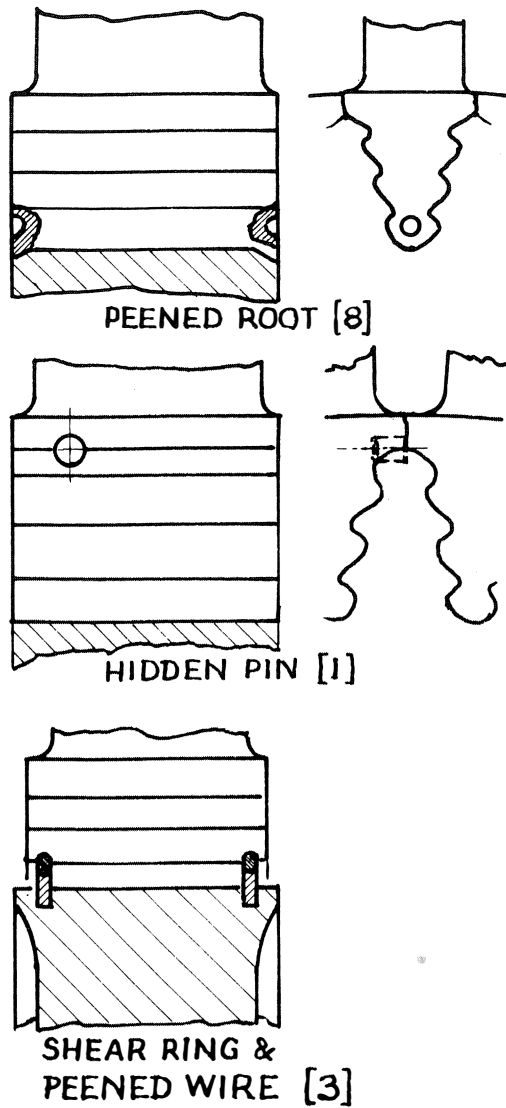


Figure 37. Locking Methods of Axial Entry Blades.

the free blade ends. Several blades are held together by one plate. Between plates gaps are provided for thermal expansion.

Using the same grading scheme for the shrouds, as was used for the root designs, a variety of shroud configurations shall be considered. The use of the same grading method does not necessarily imply that these designs have to go together.

5.1.1 Rivets with Square Cross Section

The shape of square rivets is found with drawn section blades and bar stock blades. By milling the blade material back with a straight cut, a rivet head is formed as shown in Figures 23 and 24. Holes of the same shape are punched into shroud strips.

Small tears in the plate material as a result of the punching process and the rather high stress concentrations at the four corners of the shroud after riveting, lead frequently to shroud cracks, as shown in Figure 38. If this occurs, even for one blade, generally the whole row has to be rebladed.

The design is well suited for stationary blades. Its use for rotating blades should be restricted for ultra light service (intermediate stages).

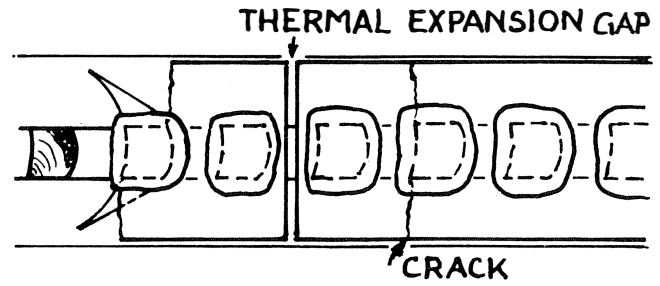


Figure 38. Shroud with "Square" Rivet.

5.1.2 Rivet with Circular Cross Section

Figure 39 shows the application of cylindrical rivets. Without special attention to the transition radius between rivet shank and vane, punched or drilled holes in shroud, counter-sunk holes and curved vane contour at tip, the design might be considered for very light to light service.

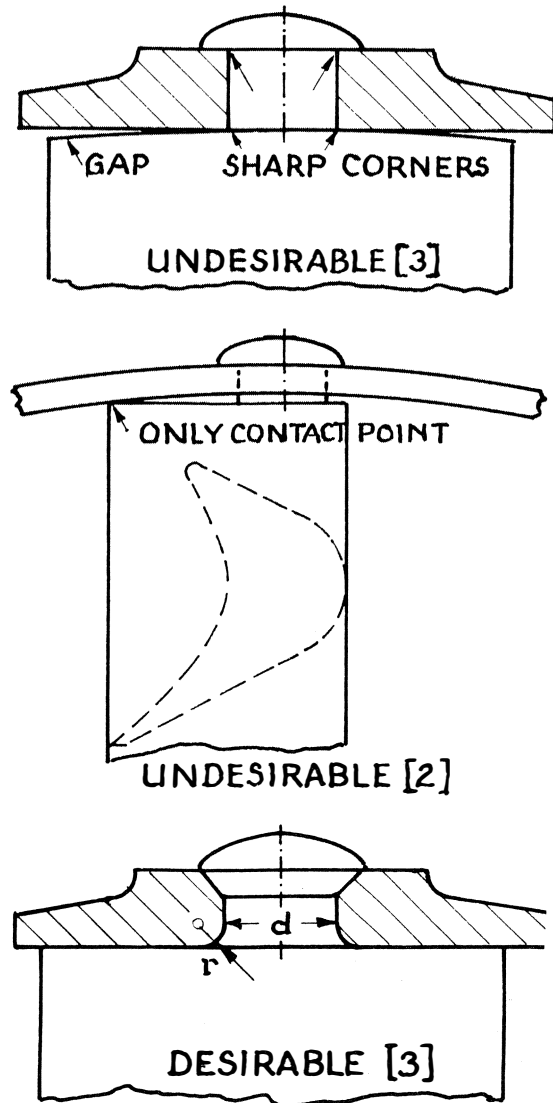


Figure 39. Shroud and Rivet Configurations.

If careful attention is given to the above mentioned detail, the design could be classified for light to medium service (intermediate and last stages, possibly lightly loaded first stage). A desirable geometry is shown at the bottom of Figure 39. Here the shroud holes are drilled, countersunk and a ratio of r/d greater than 0.1 has been provided. A satisfactory value of r/d would be 0.25 [3].

5.1.3 Integral Shroud

An example of one segment of an internal shroud is shown in Figure 31. The plate at the end is a part of the blade. The plates of several blades, which are in contact with one another, form an integral shroud.

As a group, blades are still relatively free to vibrate, because no interlocking feature between shroud plates is provided. Single blade excitation can occur only in a direction parallel to the contact surfaces as shown in Figure 40.

This high grade design is used for medium to heavy service (not well suited for first stage application without interlocking).

5.1.4 Wire-Reinforced Integral Shroud

The stiffness of an integral shroud is greatly enhanced with the insertion of wires or metal strips, which join the plates together. The inserted member is secured by either rolling or peening shroud metal over it. Prototypes of this design are shown in Figure 41.

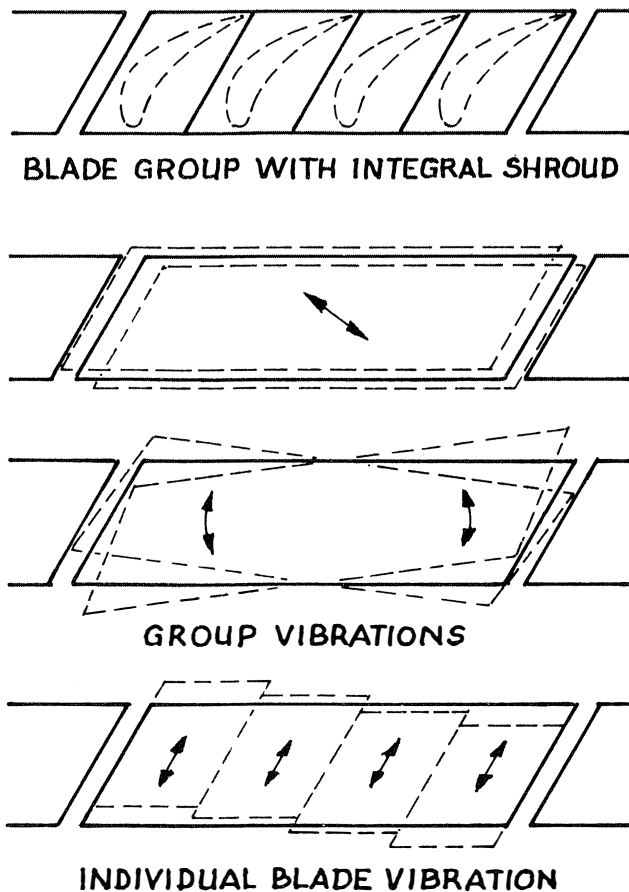


Figure 40. First Mode Vibrations of Blades with Unreinforced Integral Shrouds.

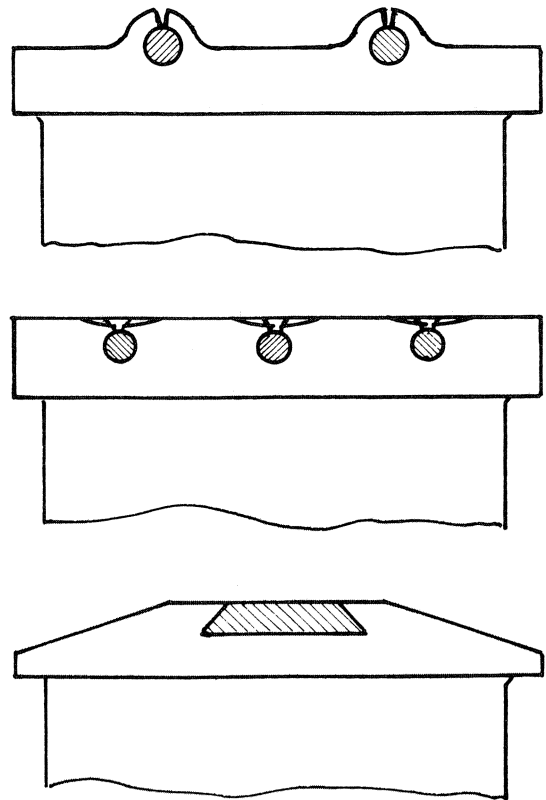


Figure 41. Reinforced Integral Shrouds.

With the interlocking feature this design is suitable for heavy service (first, second or last stage).

5.1.5 Double Shroud

A plate-reinforced integral shroud is obtained by riveting metal strips on top of the shroud, as shown in Figure 42. The arrangement is referred to as "double shroud". With this concept, maximum stiffness is achieved for blade vibrations in the circumferential direction. The design belongs in the category for very high service requirements. Its application is mainly found in first stages.

A further strengthening can be achieved by providing two rows of rivets, two per blade, as shown in Figure 43. This design, together with welded shrouds, might be assigned into the category for ultra-high service.

5.2 Special Features

In Figure 40, the movement of blade tips with unconnect-

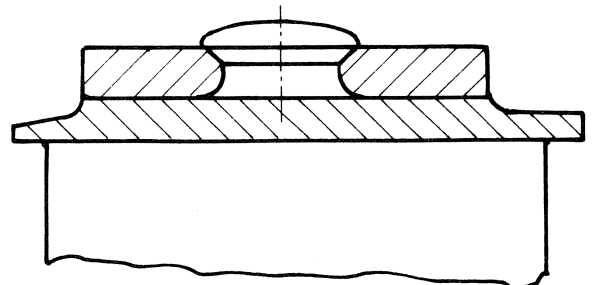


Figure 42. Double Shroud [1].

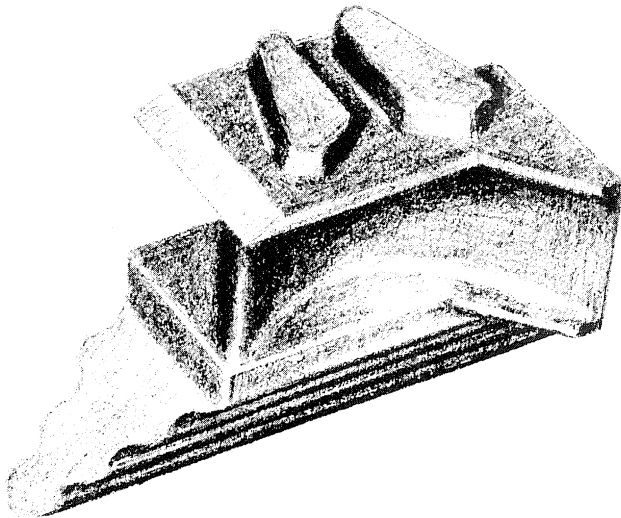


Figure 43. Axial Entry Blade with Double Rivets for Double Shroud [12].

ed integral shroud plates was demonstrated. This freedom, giving rise to high vibrational amplitudes under certain conditions, is a known source of blade failures. The same problem can exist at shroud ends, where the gap for thermal expansion is provided. Blade failures of the first or last blade in a package, held by one shroud band, may be an indication for excessive movement.

As mentioned earlier, for retaining a rectangular root platform, some blades have been designed with an overhanging trailing edge as shown in Figures 20, 43, and 44a. In another configuration, the integral shroud plate conforms with the shape of the airfoil, Figure 44b.

While these shapes are undesirable for critical root cross sections, for adjoining shroud plates they provide interlocking and damping against relative axial deflections. Such features are especially desirable for shrouded blades on either side of the shroud gap. Blades at these locations are known to have failed, due to the lack of interlocking. Among these are first stage blades with welded shrouds or double shrouds. In Figure 45, the effect of the lack of shroud interlocking is demonstrated, showing the shroud deflections of a blade row passing through a partial arc.

Another blade region, where high stress concentrations and associated failures do frequently occur, is the transition between the vane platform and the vane itself. The selection of a generous transition radius of d/r smaller than 2 or equal, where d is the maximum airfoil thickness, is recommended. This criterion is rarely met at the leading and trailing edge. An example of how this problem can be solved was shown in Figure 44a. The transition of the leading edge into the platform maintains a satisfactory radius, while the trailing edge is well supported showing rather small stress concentrations. A solution as indicated in Figure 46, however, can be quite troublesome with blade length to chord ratios l/c greater than 3. For a slightly asymmetrical shape as shown, cracks occur predominantly at the bottom of the trailing edge.

5.3 Lashing

The longest blades in a turbine, located in the low pressure or wet region, are generally twisted, using an impulse airfoil at the hub and a high reaction airfoil (airplane wing shape) at the tip. Due to the high centrifugal force, resulting

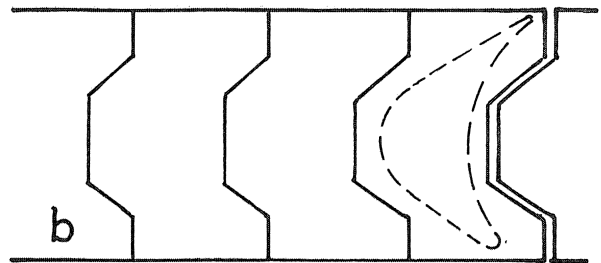
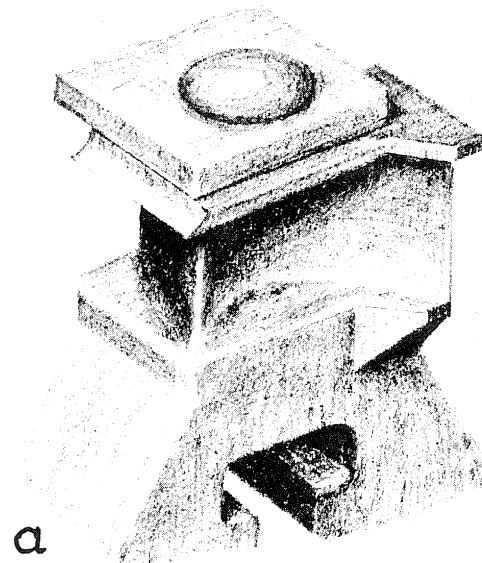


Figure 44. Blade Interlocking Features, due to a) Overhanging Trailing Edge [12], b) Overhanging Leading and Trailing Edges [13].

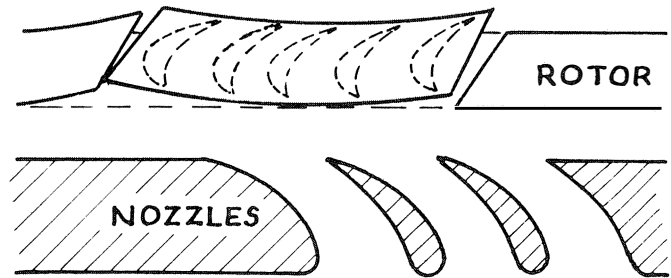


Figure 45. Shroud Deflections, due to Partial Arc Admission.

from the long blade, the root is already highly stressed and heavy shroud designs are therefore undesirable. The slender, wing shaped section of the blade, however, does in many cases require some damping.

An effective way of dealing with this problem is to insert a long wire through holes drilled in all blades at a certain radius. Any blade vibration has to overcome the centrifugal force exerted by the wire. Since this process absorbs energy, a damping effect results.

Problems with this design arise when high excitation energies exist. These can force the blades to vibrate in spite of the friction force exerted by the damping wire. Wire wear will result, and with a wire failure blade failures do occur relatively quick. Other difficulties are introduced by the free ends of the

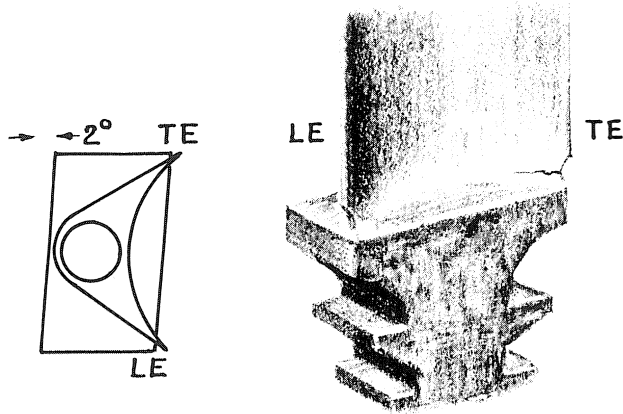


Figure 46. High Stress Concentration at Bottom of Unsupported Trailing Edge.

damping wire. These problems are similar to those caused by discontinuities in shrouds.

With this design, blade failures often originate at the wire hole. By considering a flat plate with a hole being subjected to tension, high stress concentrations exist at both sides of the hole. If the hole is drilled at an angle, as shown in Figure 47, the stress concentrations, resulting from tension and bending, become even more severe at the sharp corners.

A solution of this problem has been accomplished by providing stubs as part of the forging process on either side of the blade, (Figure 48). Holes are drilled through these stubs and a wire is inserted.

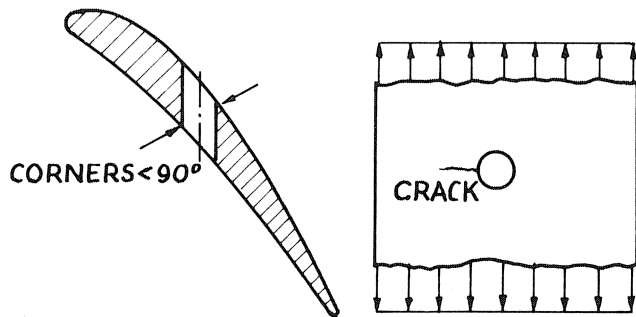


Figure 47. High Stress Concentration at Hole with Sharp Corners.

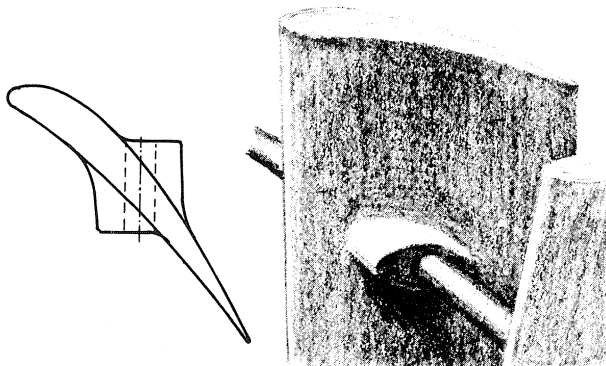


Figure 48. Stub Reinforced Hole for Damping Wire.

Another approach has been the use of short wires, long enough to join two blades, as shown in Figure 49. The difficulty of handling the free ends of a continuous wire and the thermal expansion of a rather long wire have been overcome in this manner. However, two holes instead of one are located at the same blade length, resulting in a weakening of that cross section.

Another method has been to provide stubs on either side of a blade long enough that they are touching each other. Some manufacturers have even welded the stubs of several blades together, forming packages, as shown in Figure 50. The cross section of these stubs should be elliptical rather than round, which reduces the drag to one tenth.

With increasing unit size, last stage blade failures have become a major concern with industrial turbines and turbine generators [14]. Solutions of such failures are attempted with the use of integral blade connections.

For mechanical drive turbines these connections should be wide enough axially to prevent torsional blade flutter. Longer blades may be equipped with two or even three 'floors' of these connections. At discontinuities of the lashing sections, "plug" type connections, as shown in Figure 51, might have to be provided to eliminate axial and circumferential modes of package vibrations. For turbine generators, free standing last blades with stiffening through centrifugal bending have proven to be quite successful.

CONCLUSIONS

For various types of steam turbine blades, the effect of alternating blade forces and unsteady temperatures has been reviewed with emphasis on the fatigue of roots, shrouds, and damping devices. The significance of the circumferential versus the axial component of the alternating blade forces, was

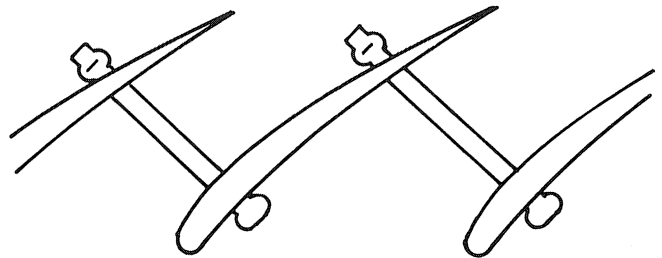


Figure 49. Zig-zag Lashing at Blade Tips.

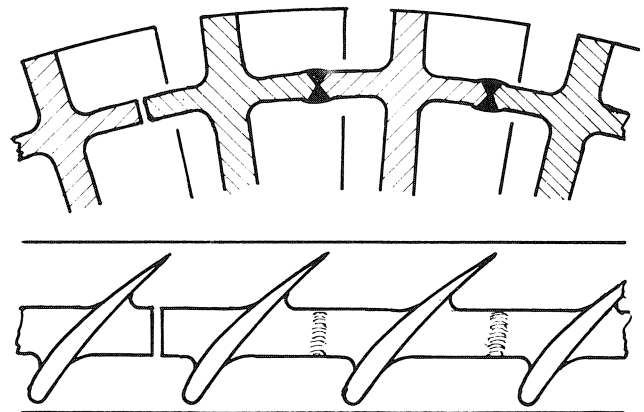


Figure 50. Welded Lashing Stubs.

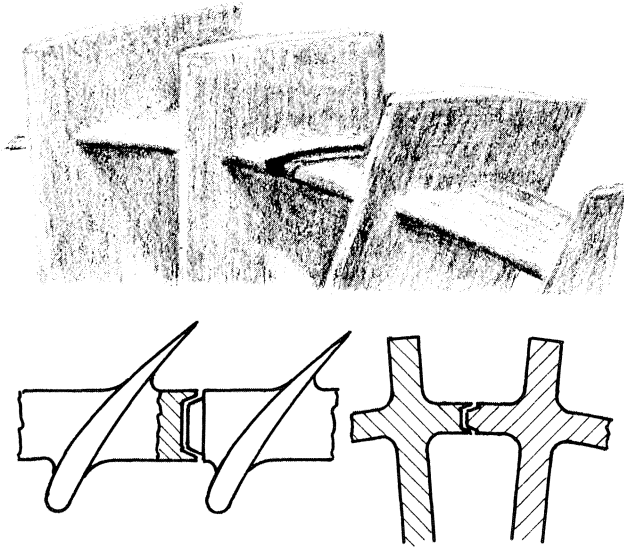


Figure 51. Interlocking Feature at Lashing Discontinuity.

considered in reference to differences of rotor stiffness in the two directions. Based on these findings, high stress regions (origins of failure) were pinpointed on circumferential cross sections of various root designs, and shapes with minimal stress were identified. Root, shroud, and damping designs were rated as to their relative strength to one another, and the findings are presented for quick reference in Appendixes I, II, and III respectively.

REFERENCES

1. Kroon, R. P.: "Impulse Turbine Blade Failures". Engineering Case Library, ELC 1003, Stanford University, Stanford, California, 1966.

2. Sohre, J. S.: "Steam Turbine Blade Failures, Causes and Corrections". Proceedings of the Fourth Turbomachinery Symposium, Texas A&M University, College Station, Texas, 1975.

3. Traupel, W.: "Thermische Turbomaschinen" (in German), Vol. II, 2nd edition, Springer-Verlag Berlin, 1968.

4. Skrotzki, B. G.: "Steam Turbines", Special Report of Power Magazine, New York, N.Y., 1962.

5. Naumann, H. G. and Yeh, H.: "Lift and Pressure Fluctuations of a Cambered Airfoil Under Periodic Gusts and Applications in Turbomachinery". Journal of Engineering for Power, Trans. ASME, January, 1973.

6. Owczarek, J. A.: "On a Wave Phenomenon in Turbines", ASME 66-GT-99.

7. Brinker, J.: "Experience with Integral ECM Rotor Blades" (in German), Siemens-Zeitschrift, 44. Jahrgang, 1970.

8. Spechtenhauser, A.: "Modern Industrial Turbine Blading", Brown Boveri Publication No. CH-T 110263E.

9. Hetenyi, M.: "Some Applications of Photo Elasticity in Turbine-Generator Design", J. Appl. Mech. 61, 1939.

10. Peterson, R. E.: "Stress Concentration Design Factors", John Wiley & Sons, Inc. New York, 1953.

11. Petermann, H.: "Construction and Elements of Turbomachinery", (in German), Springer-Verlag Berlin, 1960.

12. General Electric Publication: "Mechanical Drive Turbines", GEA-6232C, 1981.

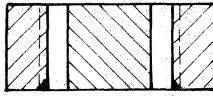
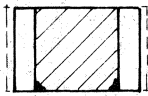
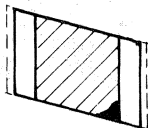
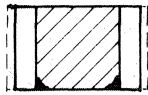
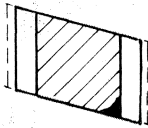
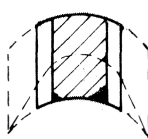

13. Dietzel, F.: "Steam Turbines", (in German), 2nd edition, Carl Hauser Verlag, Munchen, 1970.

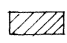
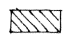
14. Höxtermann, E.: "Blade Failures of Steam Turbines", (in German), VGB Kraftwerkstechnik 59, Heft 12, December, 1979.

15. Loschge, A.: "Steam Turbine Design" (in German). Springer-Verlag, Berlin, 1967.

APPENDIX I, Rating of Root Cross Sections

<u>Service</u>	<u>Root Type</u>	<u>Cross Section</u>	<u>Stress Concentration</u>
a) Ultra heavy	Axial entry Figure 7n Section 4.4		minimal
			low in rotor shank
b) Very heavy	Pinned Figure 7j Section 4.3		very low in rotor blade

c) Heavy	Straddled Figure 7e Section 4.2		low
d) Medium	Internal groove Double T Serrated Figure 7b,c Section 4.1.2.3		medium
			high
e) Light	Internal groove T-root Figure 7a Section 4.1.2.2		medium
			high
f) Very light	Curved root cross section Figure 24 Section 4.1.2.1		very high
g) Ultra light	Drawn section Figure 23 Section 4.1.1.		ultra high

 Root shank  Rotor, Blade platforms are identical (dashed line)

APPENDIX II, Rating of Shrouds

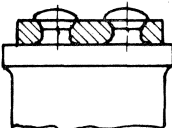
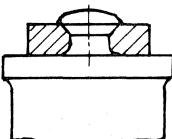
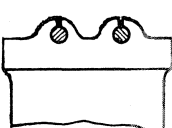
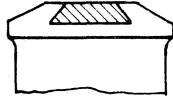
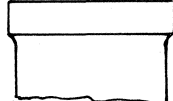
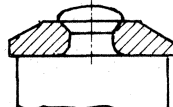
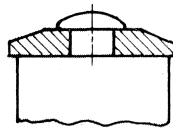
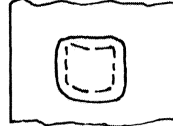
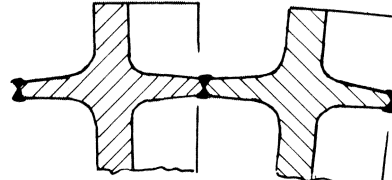
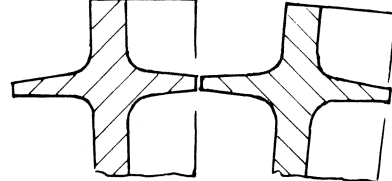
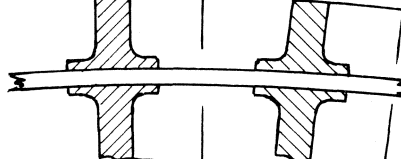
<u>Service</u>	<u>Shroud Type</u>	<u>Cross Section</u>
Ultra heavy	Double shroud & double rivet. Welded	
Very heavy	Double shroud, single rivet	
Heavy	Wire reinforced integral shroud	

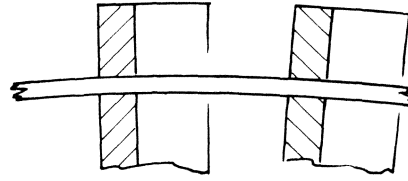
	Plate reinforced	
Medium	Integral shroud	
Light	Cylindrical rivet, drilled shroud, counter sunk	
Very light	Cylindrical rivet punched shroud	
Ultra light	Square rivet, punched shroud	

APPENDIX III, Rating of Damping Devices

<u>Service</u>	<u>Damping Type</u>	<u>Cross Section</u>
Very heavy	Integral lashing welded	
Heavy	Integral lashing	
Medium	Lashing wire with blade stubs	

Light

Hard soldered
lashing wire



Very light

Damping wire

